



**New stratigraphic and genetic model  
for the dolomitic Cretaceous Pinda reservoirs in Angola**

**Part I - The Pinda of Angola,  
an integrated lithostratigraphic approach**

**Bruno GRANIER**<sup>1</sup>

**Abstract:** The Pinda Group of the Congo basin in the northern Angolan offshore is an overall transgressive supersequence of late Aptian - ? early Cenomanian age. Due to synsedimentary salt tectonics of the underlying Loeme Salt, the original ramp arrangement is split into discrete structures corresponding to many proven, probable and possible oil and gas plays. Where the biostratigraphic information was not destroyed by pervasive dolomitization, the little that remains is not available to the general public because it is treated as proprietary data by the Sociedade Nacional de Combustíveis de Angola Empresa Pública – Sonangol E.P. Only a limited set of data containing lithostratigraphic information (e.g., some published well logs and photomicrographs of facies) is available. The aim of this paper is to give a little more information about the Pinda stratigraphy. For instance, to be formally defined, this poorly known unit required a type section, a shortcoming that is addressed here. The wireline log signatures of some regional seismic markers are documented because they are used to correlate wells and subdivide the Group into formations. The microfacies corresponding to some key electrofacies as well as the porosity types are also condensed in a microphotograph catalog. Finally, few examples of typical LoC (*i.e.*, Line of Correlation) diagrams are displayed and interpreted.

**Key-words:**

- Angola;
- Pinda;
- Albian;
- Cenomanian;
- reservoirs;
- dolomite;
- stratigraphy

**Citation:** GRANIER B. (2017).- New stratigraphic and genetic model for the dolomitic Cretaceous Pinda reservoirs in Angola. Part I - The Pinda of Angola, an integrated lithostratigraphic approach.- *Carnets Geol.*, Madrid, vol. 17, no. 4, p. 105-127.

**Résumé : Nouveau modèle stratigraphique et génétique pour les réservoirs dolomitiques du Pinda (Crétacé) en Angola. 1<sup>re</sup> partie - Le Pinda d'Angola, une approche lithostratigraphique intégrée.**- Dans le bassin du Congo, domaine maritime septentrional de l'Angola, le Groupe Pinda représente une mégaséquence globalement transgressive d'âge Aptien supérieur à Cénomaniens ? inférieur. En raison d'une tectonique salifère synsédimentaire liée au Loeme Salt sous-jacent, l'agencement d'origine en rampe est disloqué en structures individualisées correspondant à autant d'objectifs pétroliers et gaziers avérés, probables et possibles. Lorsque l'information biostratigraphique n'a pas été détruite par une dolomitisation quasi générale, le peu de données existantes n'est pas accessible au public car considéré comme propriété exclusive par la Sociedade Nacional de Combustíveis de Angola Empresa Pública – Sonangol E.P. Seul un ensemble relativement limité de données lithostratigraphiques (quelques publications de diagraphies de puits ou des photos de microfaciès, par exemple) est disponible. L'objectif de cet article est de donner un peu plus d'informations sur la stratigraphie du Pinda. Ainsi, pour être formellement définie, cette unité trop mal connue a besoin d'une section de référence, une lacune qui est corrigée ici. Les signatures diagraphiques de quelques marqueurs sismiques régionaux sont consignées parce qu'elles sont utilisées pour corréliser les puits et subdiviser le

---

<sup>1</sup> "Cátedra Franco-Brasileira no Estado de São Paulo 2015", UNESP - Universidade Estadual Paulista, Center for Geosciences Applied to Petroleum (UNESPetro), Caixa Postal 178, Av. 24 A, no. 1515, Bela Vista, CEP13506-900 - Rio Claro - SP (Brazil);  
Dépt. STU, Fac. Sci. Tech., UBO, 6 avenue Le Gorgeu, CS 93837, F-29238 Brest (France)  
[bgranier@univ-brest.fr](mailto:bgranier@univ-brest.fr)  
Department of Ecology and Evolutionary Biology, The University of Kansas, 1200 Sunnyside Avenue, Lawrence, Kansas 66045 (USA)  
[bgranier@ku.edu](mailto:bgranier@ku.edu)



Groupe en formations. Les microfaciès correspondant aux quelques électrofaciès les plus communs ainsi que divers types de porosités sont également rassemblés dans un catalogue photographique. Enfin, quelques exemples de diagrammes de corrélations graphiques présentant des puits sous forme de "Lignes de Corrélations" sont discutés et interprétés.

**Mots-clefs :**

- Angola ;
- Pinda ;
- Albien ;
- Cénomanién ;
- réservoirs ;
- dolomie ;
- stratigraphie

**Resumo: Novo modelo estratigráfico e genético para os reservatórios dolomíticos cretácicos Pinda, em Angola Parte I - O Pinda de Angola, um enfoque litoestratigráfico integrado.-** O

Grupo Pinda, Bacia do Congo, no mar afora do norte de Angola, é no geral uma supersequência transgressiva de idade neoptiana - (?) eocenomaniana. Devido à tectônica salífera sinsedimentar associada ao subjacente Sal Loeme, a rampa é dividida em distintas estruturas que correspondem a muitos plays de óleo e gás comprovados, prováveis e possíveis. Onde a informação bioestratigráfica não foi destruída por dolomitização pervasiva, o pouco que resta não está disponível para o público em geral; é tratado como dados proprietários pela Sociedade Nacional de Combustíveis de Angola Empresa Pública – Sonangol E.P. Somente um conjunto limitado de dados contendo informação litoestratigráfica está disponível (e.g., alguns perfis de poços publicados e fotomicrografias de fácies). O objetivo deste artigo é oferecer um pouco mais de informação sobre a estratigrafia do Grupo Pinda. Por exemplo, para ser formalmente definida, esta unidade pobremente conhecida deveria ter uma seção tipo, uma lacuna que é aqui apontada. As assinaturas em perfis de poços de alguns marcadores sísmicos regionais são documentados, uma vez que eles têm sido usados para correlacionar poços para subdividir o grupo em formações. As microfácies correspondentes a algumas eletrofácies-chave, assim como os tipos de porosidade, são também reunidas em um catálogo fotomicrográfico. Finalmente, alguns exemplos de típicos diagramas LoC (*i.e.*, Linha de Correlação) são apresentados e interpretados.

**Palavras-chave:**

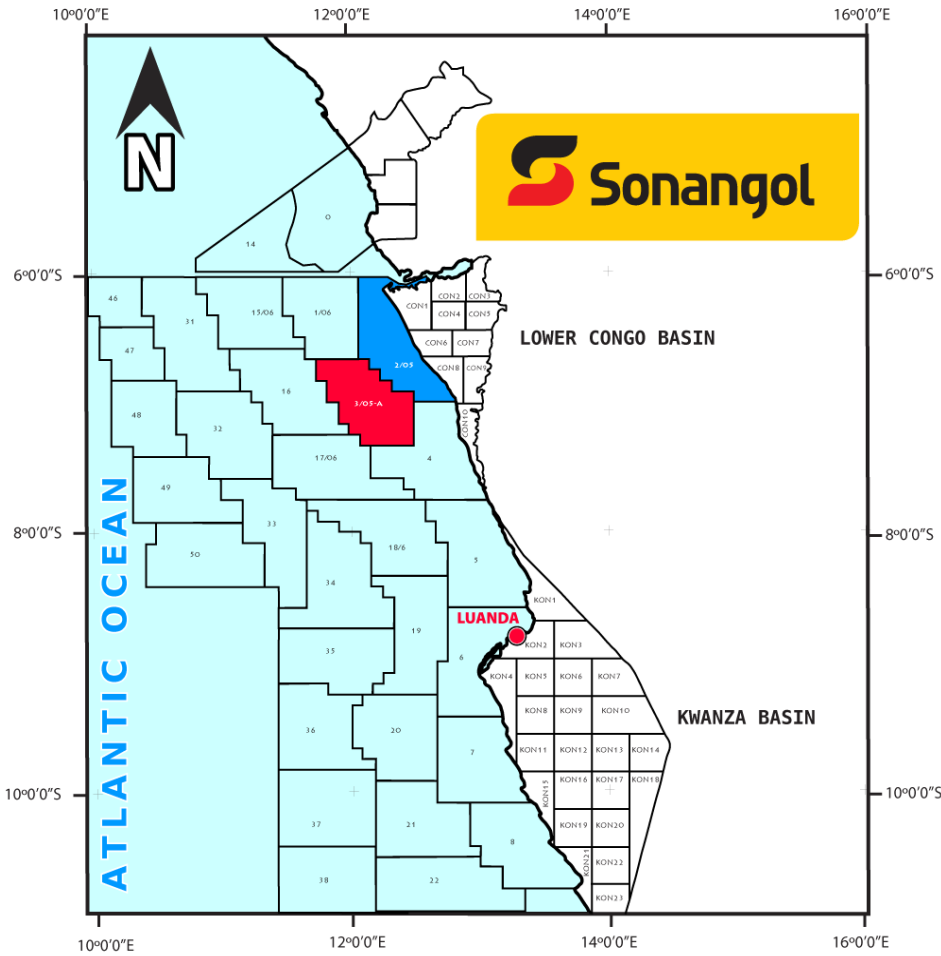
- Angola ;
- Pinda ;
- Albien ;
- Cénomanién ;
- réservoirs ;
- dolomie ;
- stratigraphie

## 1. Introduction

In the Congo basin of northern Angola, following the early Aptian syn-rift episode characterized by the Loeme Salt deposition, the first post-rift episode spanning the late Aptian - ? early Cenomanian interval corresponds to the overall transgressive supersequence referred to as the Pinda Group (Fig. 1). The latter consists from base to top of immature siliciclastic sediments passing gradually to shallow-water limestones (commonly extensively dolomitized), that in turn pass into hemipelagic marl-limestone rhythmites and deeper-water marls. Another post-rift episode, which overlies the Pinda, corresponds to the dominantly shaly Iabe Group. This last group, ranging in age from the Cenomanian to the Eocene, was affected by multiple intraformational unconformities. The lower part of the Pinda, which has locally proved to host oil and gas reservoirs, has been extensively explored and a significant number of wells were drilled, with some cores recovered. The integrated lithostratigraphic approach documented below is intended to provide support and guidance to junior geologists working on the Pinda or similar formations, *i.e.*, a sort of "starter kit".

## 2. Rough sketch of the Pinda stratigraphy

As a practical stratigrapher I have always developed holostratigraphic approaches, *i.e.*, holistic approaches of stratigraphy, to address most questions and more specifically reservoir and seal issues that are relevant for the oil and gas industry. The Greek prefix *hólos* indicates that ideally all approaches and techniques of stratigraphy should be involved to result in a balanced and integrated synthesis. However, in the case studied, there are several limitations. For instance, no biostratigraphic data has been presented for Angolan fields. Pervasive dolomitization is responsible for the destruction of most calcareous microfossils in the Pinda interval. However, comparison with time-equivalent and less diagenetically altered units in Angola (DSDP Site 364, off the Kwanza basin, see KOCHHANN *et al.*, 2013), in Congo (Sendji Formation of the Congo basin, see MASSE, 1995) and in Brazil (Riachuelo Formation of the Sergipe-Alagoas basin, see KOUTSOUKOS *et al.*, 1991, *inter alia*) corroborates the late Aptian to ? early Cenomanian ages. It is worth mentioning that published records of calcareous microfossils are anecdotal. For instance, ROMANES



◀ **Figure 1:** Location of Blocks 2 (blue) and 3 (red) in Angola's concessions (excerpt from GAD201501-DMC0001-I-A).

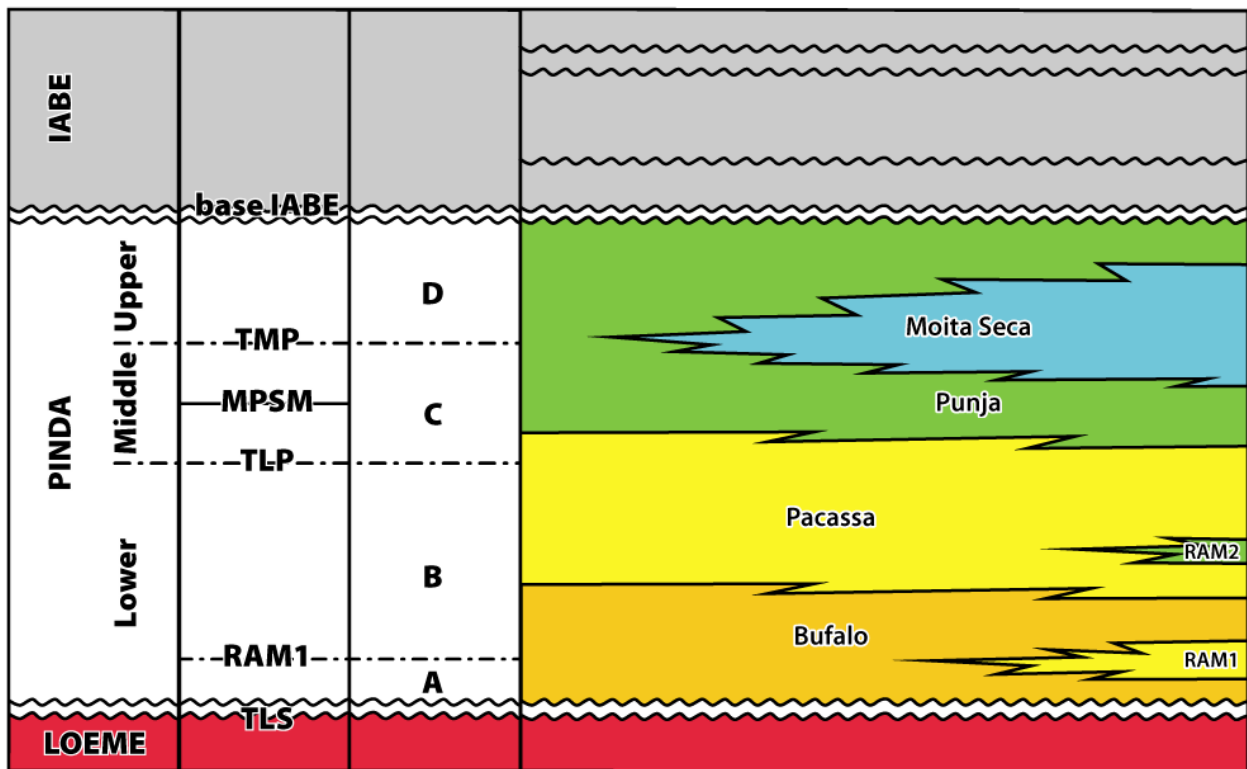


**Figure 2:** Pinda stratigraphic nomenclature (formations, members, facies, and key surfaces).

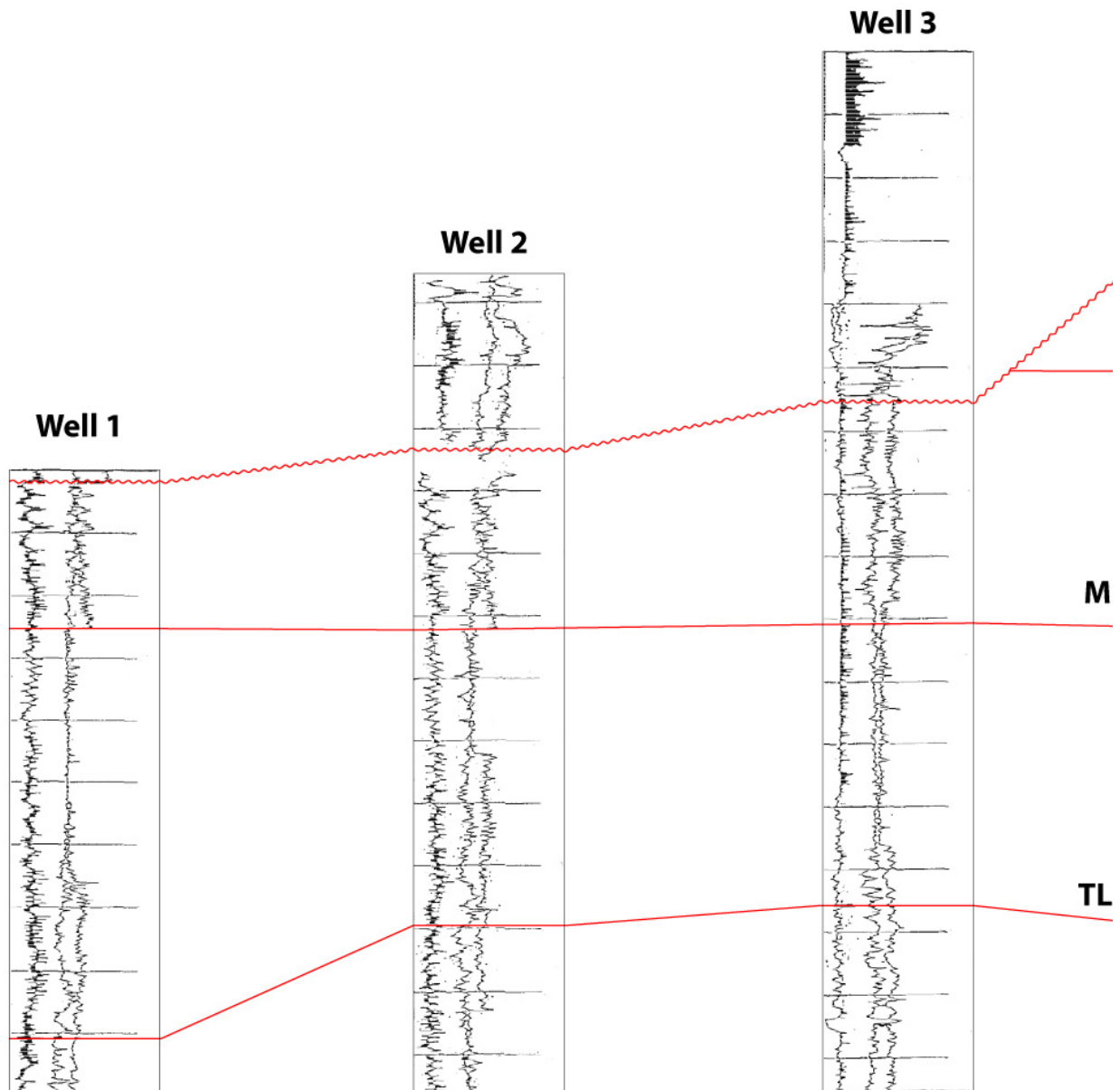


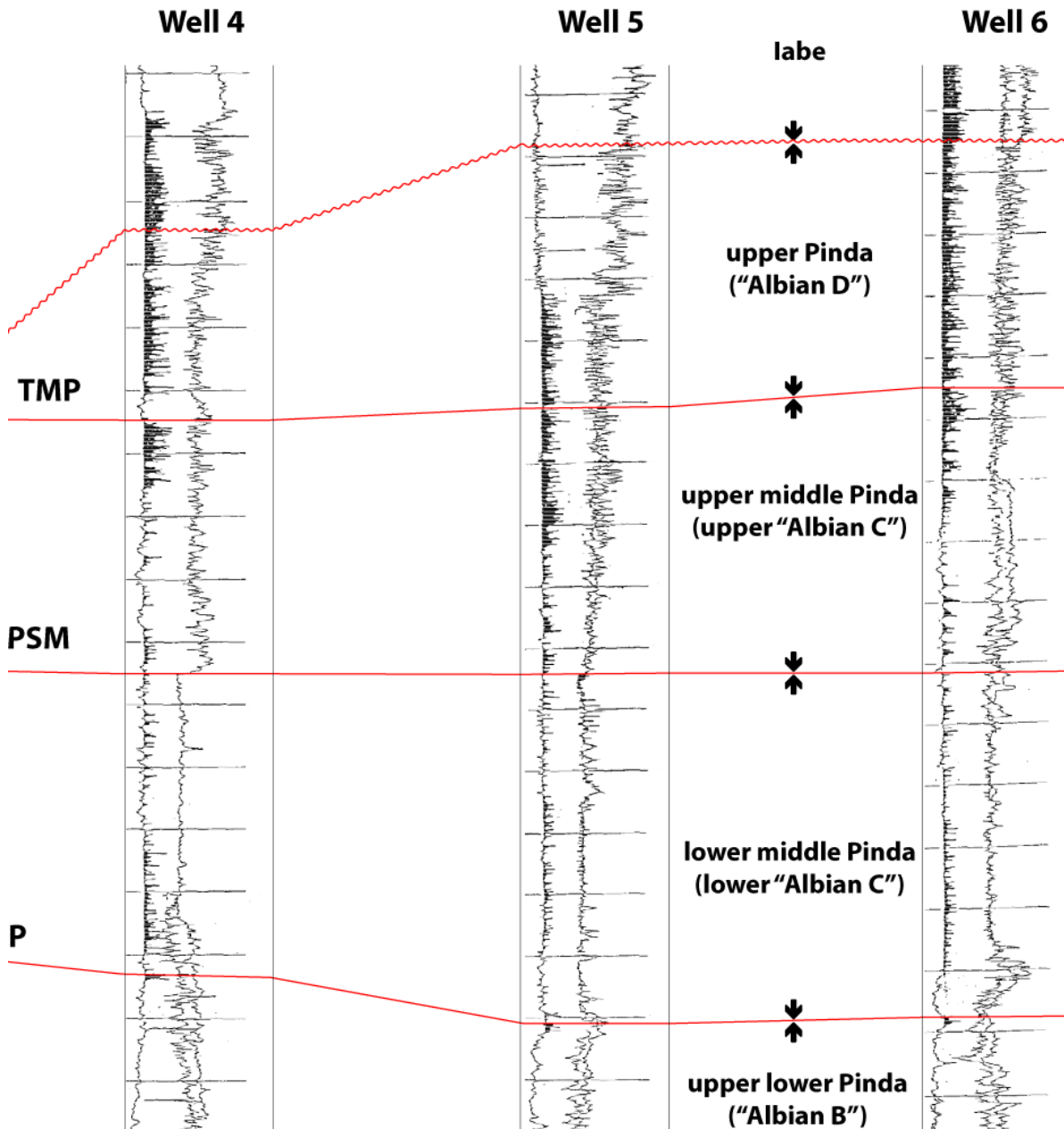
**Figure 3:** Wells 1 to 6, with base Iabe, TMP, MPSM and TLP markers, that frame the upper Pinda, upper middle Pinda and lower middle Pinda.

For confidentiality purposes the names of wells as well as the depth, GR, RhoB, and NPhi scales are not provided [RhoB and NPhi scales are reversed. From left to right, the RhoB scale runs from high to low, and the NPhi scale runs from low to high].

(1916) described "*Lithothamnion angolense*" from material collected by J.W. GREGORY near Lobito (Benguela Province). This calcareous alga, which is a synonym of *Marinella lugeoni* PFENDER, 1939, has no stratigraphic value (GRANIER & DIAS-BRITO, 2016). More recently, FERRÉ and GRANIER (2001) documented the occurrence of the planktonic foraminifer *Favusella washitensis* (CARSEY), an Albian-Cenomanian species (Pl. 1, figs. 10-11), associated with exceptionally well-preserved reoecrinids, *i.e.*, planktonic stemless microcrinoids, from middle Pinda cores of the Bagre 1 well (Block 2, offshore Angola). Alternatively, palynology, which involves the study of organic

microfossils, was used to address biostratigraphic issues. Unfortunately, these studies are proprietary, and therefore unavailable to us. Consequently, we shall focus solely on lithostratigraphy.

The lower boundary of the Pinda (Figs. 2 & 4) with the Loeme Salt has never been observed as a normal stratigraphic contact but most often as a gravitational gliding surface that forms the sole of huge sedimentary rafts. In fact, the Pinda carbonate ramp system is split into a mosaic of NNE-SSW elongated structures, a few kilometres wide and several kilometres long, which contain many prospects or discrete oil and gas fields, usually



named after fish in Block 2 (e.g., Lombo for "loin" and Sulele for "sole") and after mammals in Block 3 (Palanca for "antilope" and Búfalo for "buffalo").

The upper boundary of the Pinda (Figs. 2-3) with the Iabe Group is an unconformity, commonly interpreted as multiple submarine erosional surfaces cutting more or less deeply into the Pinda (locally down to the middle Pinda). Therefore the Pinda can be treated as a lithostratigraphic unit, either an UBU, *i.e.*, Unconformity-Bounded Unit or an alloformation.

In addition, because the Pinda is also very thick, e.g., reaching 860 m in thickness at Lombo East 1 well in the Block 2 in the Angolan offshore, it may be --and at one time was-- divided into subunits. **elf** --also known as SNEA(P)--, the former operating company on Block 2 in the Angolan offshore, subdivided the Pinda into four

facies-based formations derived from STARK (1991; see EICHENSEER *et al.*, 1999): Bufalo, Pacassa, Punja and Moita Seca units, that we shall not refer to as "formations" but as "facies", and four time-based formations (see EICHENSEER *et al.*, 1999): "Albian" A, B, C, and D. On the other hand, **Total**, the former operating company of some fields on the neighbouring Block 3, subdivided it into three time-based formations (STARK, 1991): lower Pinda (equivalent to Albian A and B), middle Pinda (equivalent to Albian C) and upper Pinda (equivalent to Albian D), each bounded by seismic markers. Thus, the TLP-Top Lower Pinda (Figs. 3-4) and the TMP-Top Middle Pinda (Fig. 3) were primarily defined by seismic markers before they were identified on well logs and cores. The MPSM (Middle Pinda Seismic Marker, Fig. 3) within the middle Pinda and two

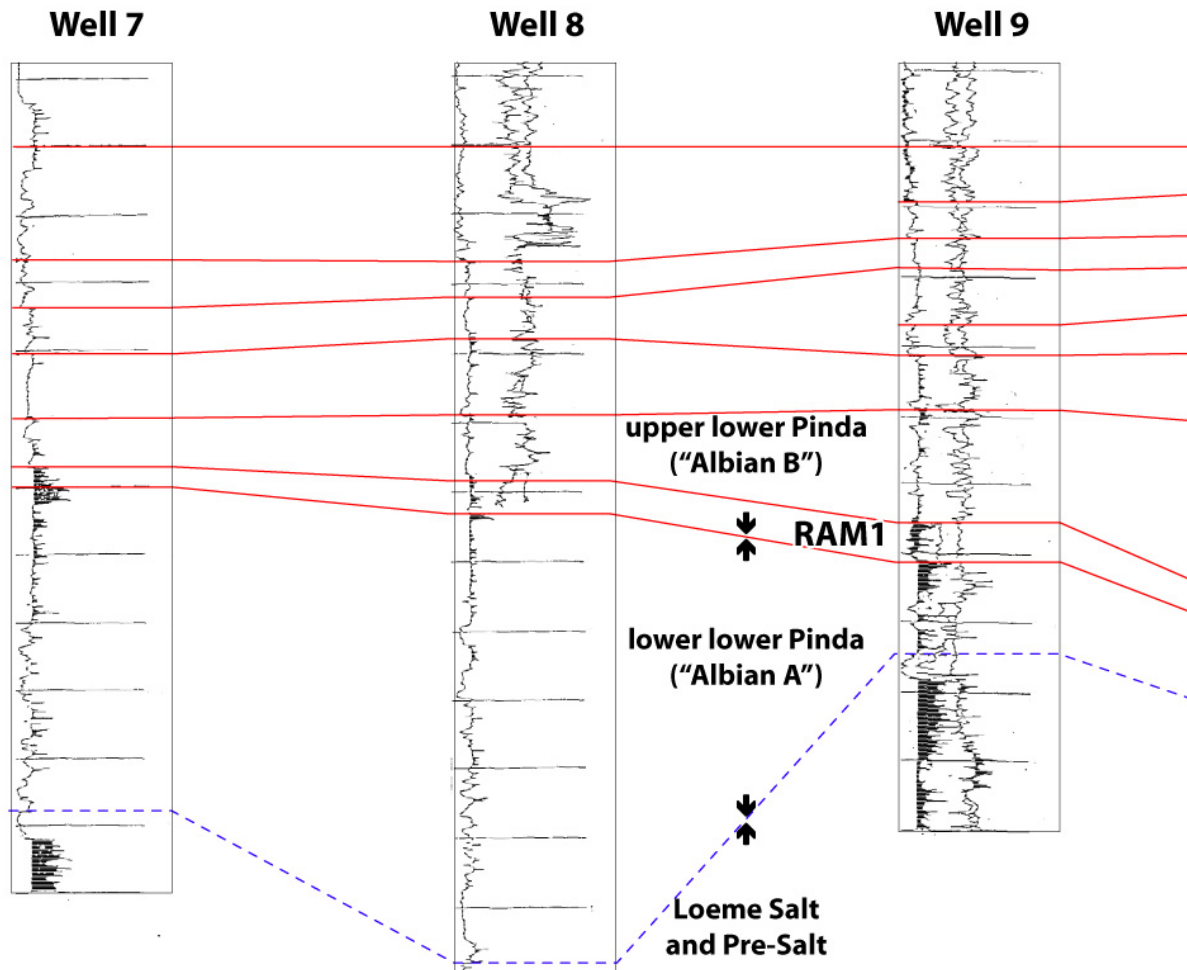


**Figure 4:** Wells 7 to 12, with RAM 1 and Top Salt, which frame the lower lower Pinda.

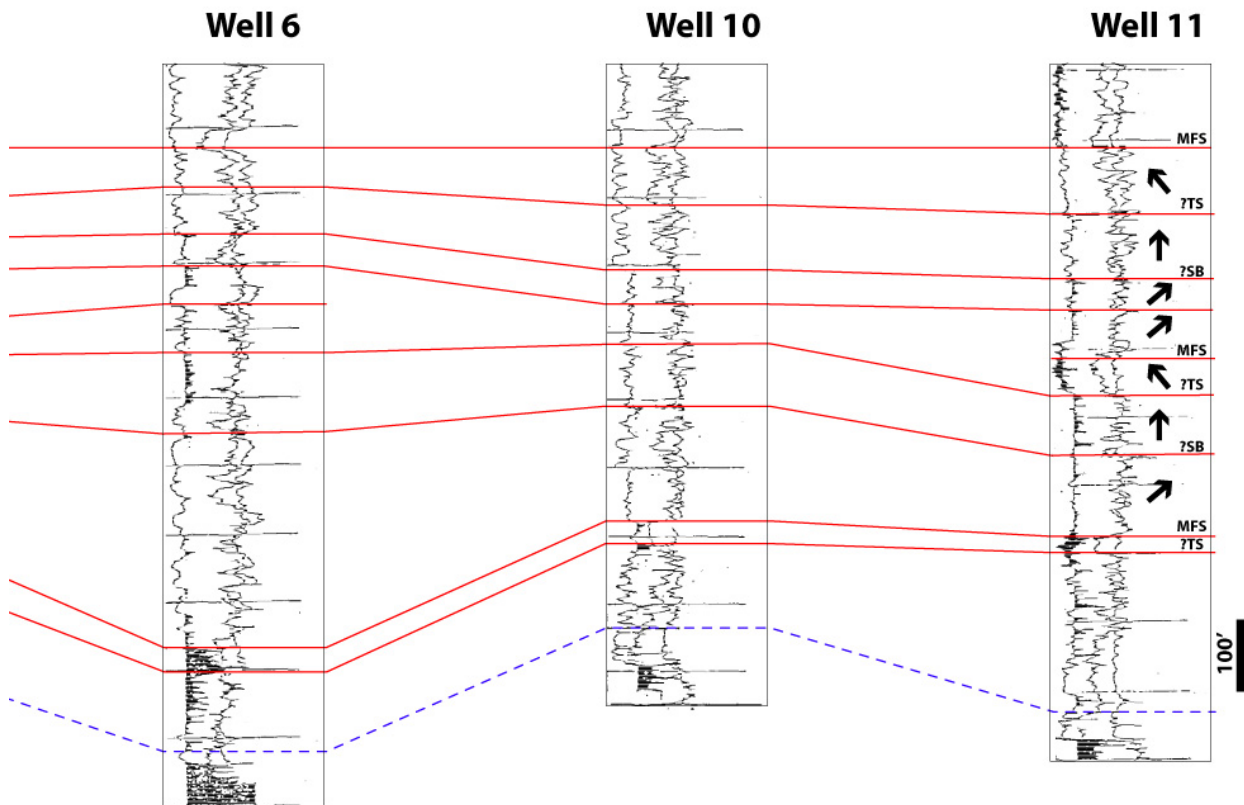
RAM's (RadioActive Markers), detected on the gamma ray log within the lower Pinda, allow further subdivision of these units, *i.e.*, the lower RAM or RAM1 (Fig. 4) marks the boundary of the Albian A and B.

The reference section selected for the Pinda and its subunits is the Lombo East 1 well because key information from it has already been published (STARK, 1991, p. I-55; the few new depth ascriptions are hereafter indicated by asterisks):

- from 9425 ft to 8499 ft\* (base of the lower RadioActive Marker or RAM1), the "Albian A" or lower part of the lower Pinda: its Bufalo facies consists dominantly of silty or sandy coarsely-crystalline dolomites with some sandstones;
- from 8499 ft\* to 7548 ft (Top Lower Pinda), the "Albian B" or upper part of the lower Pinda with the upper RadioActive Marker or RAM2 at 8017 ft\*: its Pacassa facies records an upward gradient from coarsely to finely crystalline dolomites;

- from 7548 ft to 6910 ft (Top Middle Pinda), the "Albian C" or middle Pinda: its Punja facies grades upward from finely crystalline dolomites to argillaceous limestones, with local occurrences of chert near an intra-Middle Pinda Seismic Marker at 7225 ft\*;
- from 6910 ft to 6604 ft (Base Iabe), the "Albian D" or upper Pinda: its Moita Seca facies consists dominantly of argillaceous limestones and marls.

Prior to seeing the actual rock from the sub-surface, the explorationist gets a seismic image that, with some technical support from geo-physicists, helps visualize potential reservoirs and their seals, as well as some seismic markers. When the well is drilled, geologists will then identify these features on a set of wireline logs (gamma ray (GR), conventional or spectral or both, neutron porosity (NPhi), bulk density (RhoB), *inter alia*). They will also analyze drill bit cuttings of rock to better understand the succession of lithologies. Eventually a sedimentologist will have access to a core and the macrofacies, then to a thin-section and the microfacies.



### 3. Seismic and wireline log markers

The seismic markers (TMP, MPSM, TLP) can be easily correlated over Blocks 2 and 3 of the lower Congo basin. They are also easy to pick on well logs due to the specific GR signatures above and below the marker and a porosity break at the marker. Because they are located at trend reversals, they are assumed to correspond to maximum flooding events. As a consequence of this, the Albian C (or middle Pinda), for instance, is not an unconformity-bounded unit.

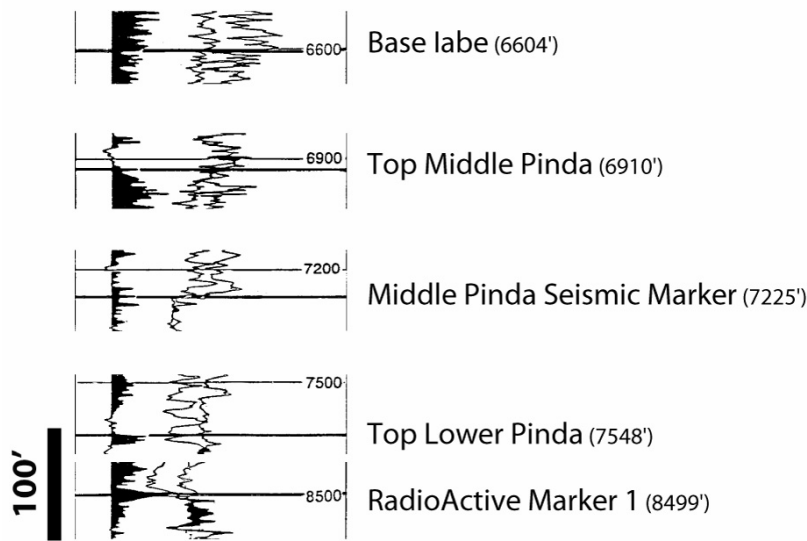
Because these markers are located in non-reservoir intervals, either in Moita Seca or Punja facies, no core were recovered from these intervals. However, drill cuttings may be examined instead. The lithology is usually inferred directly from the electrofacies only.

### 4. Electro-, macro-, and microfacies

**A)** Wireline logs may be used separately. The GR values are low in the dolosparites, in the anhydrites of the Loeme Salt or anhydrite as fracture fill, and in cherty layers; high values are found in silty-sandy dolosparites and arkosic

sandstones, which are rich in mica and feldspar, and in organic-rich dolomicrites. The RhoB tool measures the density of rock in the subsurface. It tends toward a  $2.71 \text{ g/cm}^3$  value for calcite (limestones),  $2.64 \text{ g/cm}^3$  for the cherts and siliciclastic-rich layers,  $2.88 \text{ g/cm}^3$  for the dolomitic layers, either dolomicrites or dolosparites, and  $2.98 \text{ g/cm}^3$  for anhydrite of the Loeme Salt or across anhydrite filled open fractures (Pl. 4, figs. 4-5). The presence of porosity will decrease these values read by the tool.

According to Phil SALVADOR (personal communication, June 14, 2017), "the NPhi curve represents a conversion of the raw neutron data from the neutron tool, converted to read as a porosity curve. It is calibrated to read "correct" porosity in an assumed lithology and assumed pore-filling fluid. These are commonly limestone and sea water, respectively. Formations of different lithology, and pore fluids (e.g., oil or gas) will yield incorrect apparent porosity, and corrections must be made". NPhi values vary significantly from very high in vuggy dolosparites, to high in regular dolosparites and sandstones, to low in dolomicrosparites, and they are equal to zero in some tight



◀ **Figure 5:** Zooming in on the Lombo East 1 Pinda markers.

For confidentiality purposes the GR, RhoB, and NPhi scales are not provided [RhoB and NPhi scales are reversed. From left to right, the RhoB scale runs from high to low, and the NPhi scale runs from low to high].

limestones, or even negative (depending upon tool model), in anhydritic intervals.

**B)** Wireline logs may also be used in combination. Local experience indicates that a low GR value combined with a RhoB value tending toward 2.64 g/cm<sup>3</sup> point to cherts. When the RhoB value tends toward 2.88 g/cm<sup>3</sup> or 2.98 g/cm<sup>3</sup> the pair of logs points to dolosparites or anhydrite, respectively. The NPhi values will then help to discriminate the porous dolosparites from the tight anhydrite. A high GR value combined with a RhoB value tending toward 2.64 g/cm<sup>3</sup> points to arkosic "radioactive" sandstones and sandy dolosparites. A high GR value combined with a RhoB value tending toward 2.88 g/cm<sup>3</sup> points to organic-rich dolomiticrites.

In practice, however, there are a number of side problems related to the complex mineralogical nature of the reservoir rock, its porous network and the fluids inside the porosity. For instance, local occurrence of gas at the top of some oil reservoirs may significantly shift the RhoB curve towards lighter values (see Fig. 6, for instance); gas will also slightly shift the NPhi cur-

ve towards a low porosity reading. According to R.E. BALLAY (personal communication, March 1, 2017) "In most cases the gas effect on the NPhi will be larger than the gas effect on the RhoB. This is because the NPhi reads deeper into the formation than does the RhoB, and so mud filtrate flushing - which diminishes the gas presence, and thus diminishes the gas effect - will often be greater on the NPhi than on the RhoB".

Dolomites generally have better petrophysical properties (porosity and permeability) in terms of reservoir than the limestones (see some examples below). Dolomitization is probably the reason why Angolan Pinda reservoirs are better than those of the Congolese Sendji or the Brazilian Riachuelo. In theory, the replacement of calcite by dolomite in a closed system should result in an increase of the porosity by approximately 13% (with an initial volume of calcite equal to 100% and a final volume of dolomite equal to 86.8%), but it would be only some 6% for the replacement of aragonite by dolomite, as expressed in the following formula and tables.



	Calcite (CaCO <sub>3</sub> )	Dolomite (CaCO <sub>3</sub> , MgCO <sub>3</sub> )
number of moles	2	1
molar mass (g)	100.087	184.401
density (g/cm <sup>3</sup> )	2.711	2.876
volume* (cm <sup>3</sup> )	73.84	64.12
ratio (volumes)	100	86.8

\* the computed volumes result from the number of moles multiplied by the molar mass and divided by the density.

	Aragonite (CaCO <sub>3</sub> )	Dolomite (CaCO <sub>3</sub> , MgCO <sub>3</sub> )
number of moles	2	1
molar mass (g)	100.087	184.401
density (g/cm <sup>3</sup> )	2.93	2.876
volume* (cm <sup>3</sup> )	68.32	64.12
ratio (volumes)	100	93.8

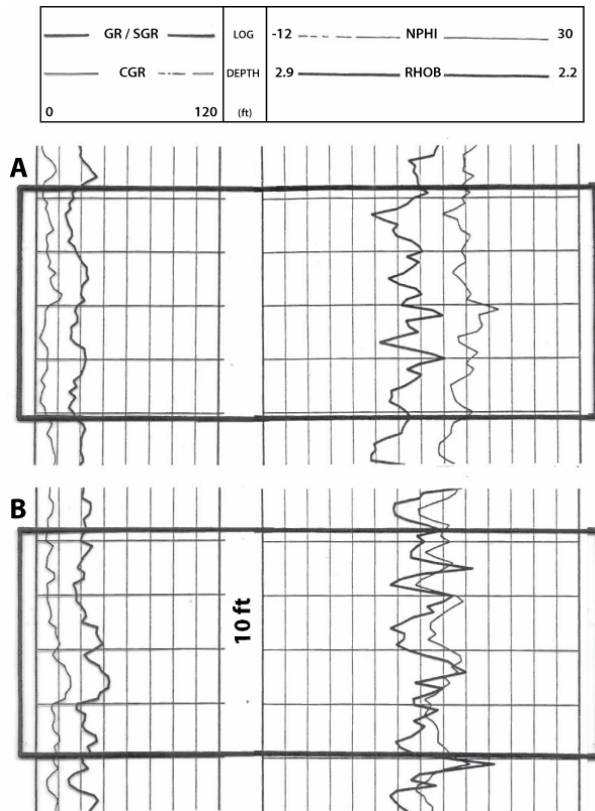


**Figure 6:** Electrofacies of a fine dolosparite, dolograinstone, oil bearing in black box A and gas bearing in black box B. For confidentiality purposes the names of wells and the depth scales are not provided.

Porosity created by calcite-to-dolomite replacement is mostly intercrystalline (Pl. 4, figs. 3, 9 & 12). The size of resulting dolomite crystals is closely connected to that of the replaced mud or grains: dolomicrite for the mudstone matrix of mud-supported fabrics and dolosparite for the grain-supported fabrics. The sizes of the pore throats are directly related to those of the surrounding dolomite crystals: dolomicrites (former mudstones) have low permeability values whereas some dolosparites (former grainstones) may be called "super-K zones" because they reach very high permeability values.

In dolomite facies, high porosity is mostly found in intervals with vuggy porosity. Vugs resulting from the dissolution of calcitic remains after dolomitization may be well-connected in dolosparites or poorly-connected in dolomicrites. Intracrystalline porosity ("Russian-doll" rhombic crystals) may add some more porosity (Pl. 2, figs. 16-18; Pl. 4, fig. 15; Pl. 6, fig. 3). Anhydrite commonly occurs in dolomite facies as a late cement in vugs. This adversely impacts porosity and permeability, which is reflected in porosity and density log values.

The combination of petrographic observations using a standard polarizing microscope with transmitted light, crossed polars, reflected light with a "white card" (Pl. 2, figs. 3, 6, 9, 12, 15 &

18), eventually supplemented by cathodoluminescence analyses (Pl. 6, figs. 2, 5, 8, 11, 14-15 & 17-19; Pl. 7, figs. 2, 5, 8, 11, 14 & 17), allows discrimination of dolomite replacement (reddish brown, locally with inclusions) leading to a porosity increase from late dolomite (dull), calcite (orange and yellow) and anhydrite (non-luminescent) cementations leading to a porosity decrease.

The section below documents some typical electrofacies displays (useful for "quick look" log interpretations, e.g., see BALLAY, 2014) with a summary of their petrophysical and petrographical characteristics. The corresponding microfacies are illustrated in an attached set of plates (Pls. 1-7).

- Dolomicrosparite or dolomudstone (Fig. 7): the gamma ray (GR) values are relatively high (45 API) and the neutron porosity (NPhi) and bulk density (RhoB) curves are widely separated. The measured porosity is about 6% related to the matrix alone. Permeability is very low. The primary texture was a mudstone and the fabric was mud-dominated (Pl. 7, fig. 9).

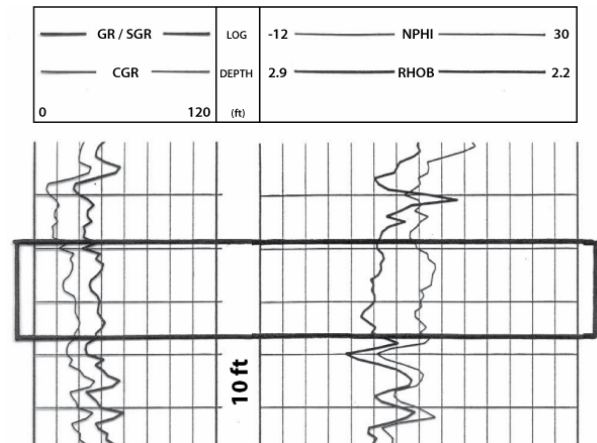


**Figure 7:** Electrofacies of a dolomicrosparite, dolomudstone (in the black box).

- Dolomicrosparite or dolowackestone (Fig. 8): the GR values are high (70 API) and the NPhi and RhoB curves are widely separated. The measured porosity is about 15%, corresponding to the matrix and to non-touching vugs (after dissolution of bioclasts). Permeability is very low. The primary texture was bioclastic wackestone, with phosphatic remains, and the fabric was again mud-dominated (Pl. 5, figs. 3 & 6).
- Fine dolosparite or dolograinstone (Fig. 6.A): the GR values are relatively low (30 API) and the NPhi and RhoB curves are widely separated. The measured porosity is about 12% and may be mainly (? solely) intercrystalline. Permeability is fair. The primary texture was a fine-grained (? peloidal) grainstone and the fabric was grain-dominated. With the gas effect, the RhoB curve is shifted to lower



values and eventually overlies the NPhi curve (Fig. 6.B).

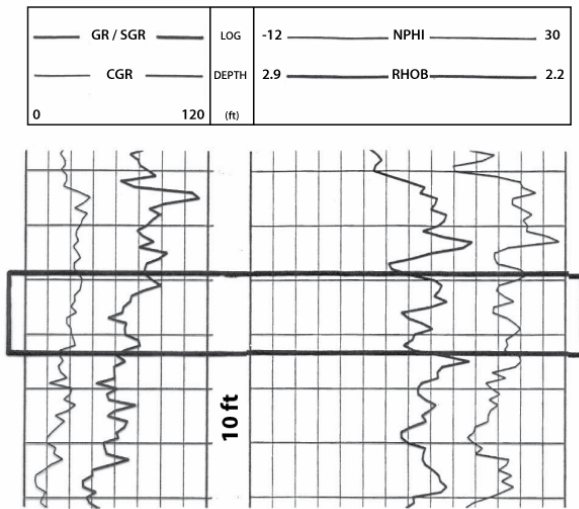


**Figure 8:** Electrofacies of a dolomicrosparite, dolograinstone (in the black box).

- Coarse dolosparite or dolograinstone (Fig. 9): the GR values are very low (15 API), NPhi and RhoB curves are separated in both the water- or oil-bearing intervals, but separation is much less in the oil-bearing interval. The measured porosity is about 24% and may be related to both the intercrystalline network and molds after the larger coated grains. Permeability is fair. The primary texture was a coarse-grained ooidal grainstone. Anhydrite commonly occurs as a late cement in vugs, impacting both density and porosity logs.

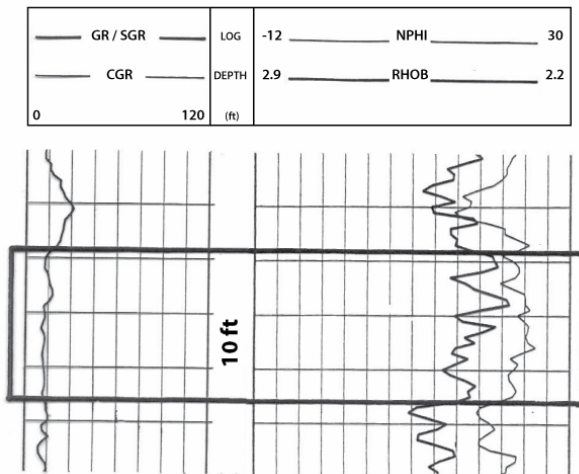


**Figure 9:** Electrofacies of a coarse dolosparite, dolograinstone (in the black box).

- Sandy dolosparite or dolograinstone (Fig. 10.A): the GR curve values are relatively low to relatively high (30 to 45 API). The RhoB curve approximately overlies the NPhi curve. The measured porosity ranges from 9 to 15% and is associated with the intercrystalline network. Permeability is fair. The primary texture is a coarse-grained sandy grainstone (Pl. 5, fig. 16).

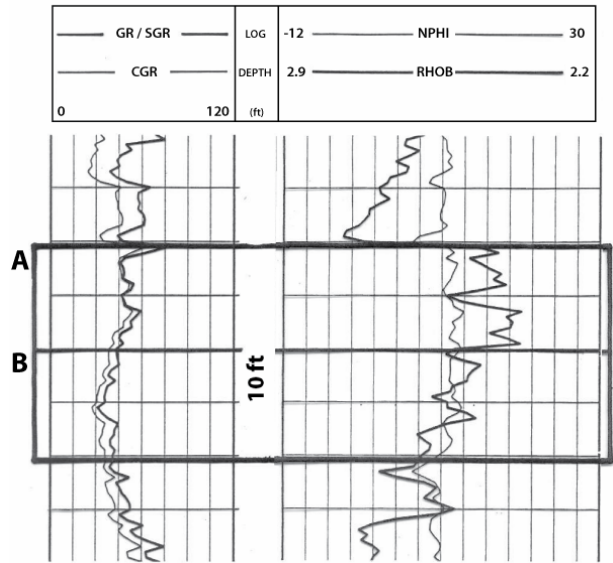


**Figure 10:** Electrofacies of a sandy dolosparite, dolograinstone, in black box A, and of a dolomitic sandstone, in black box B.

- Dolomitic sandstone (Fig. 10.B): the GR curve values are relatively high (45 API). The RhoB and NPhi curves are widely separated except for a single point where they overlie each other. The measured porosity is about 15% and is associated with the intergranular network. Permeability is fair.

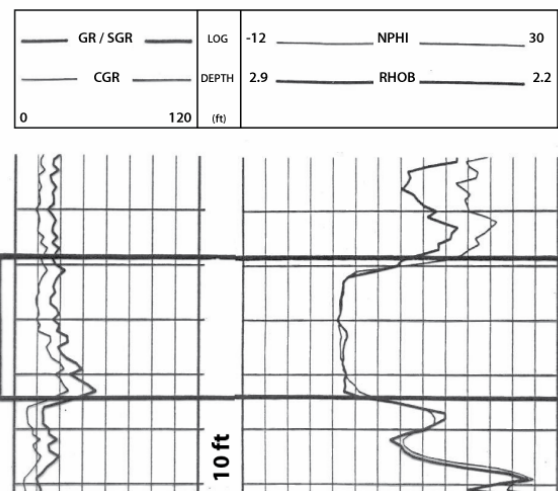


**Figure 11:** Electrofacies of a limestone (in the black box).

- Limestone (Fig. 11): the GR curve values are relatively low (30 API). The RhoB curve tends toward 2.71 g/cm<sup>3</sup> and the NPhi curve overlies it. The measured porosity is less than 3% with almost zero permeability. In this case, the microfacies corresponds to an ? oncolidal floatstone with a bioclastic-ooidal wackestone matrix.

Besides "quick look" log interpretations, some computer programs allow automatic computation of approximate lithologies (e.g., STARK, 1991; MATHIS, 1993, *inter alia*). For example, the lithologies of the four wells (A, B, C, and D) computed



for each 50-foot interval are displayed below (Fig. 12). These wells are arranged on a West to East transect (from left to right). Correlations made using either seismic or radioactive markers document some discrepancies. For example, the interpretation of the logs for the middle and upper Pinda of the second well westward (*i.e.*, well 12) suggests more shaliness than expected. The quality of the interpretations may vary from one well to the other because they rely on too many factors including the generation of the tools used or the formation fluids.

### 5. Correlations

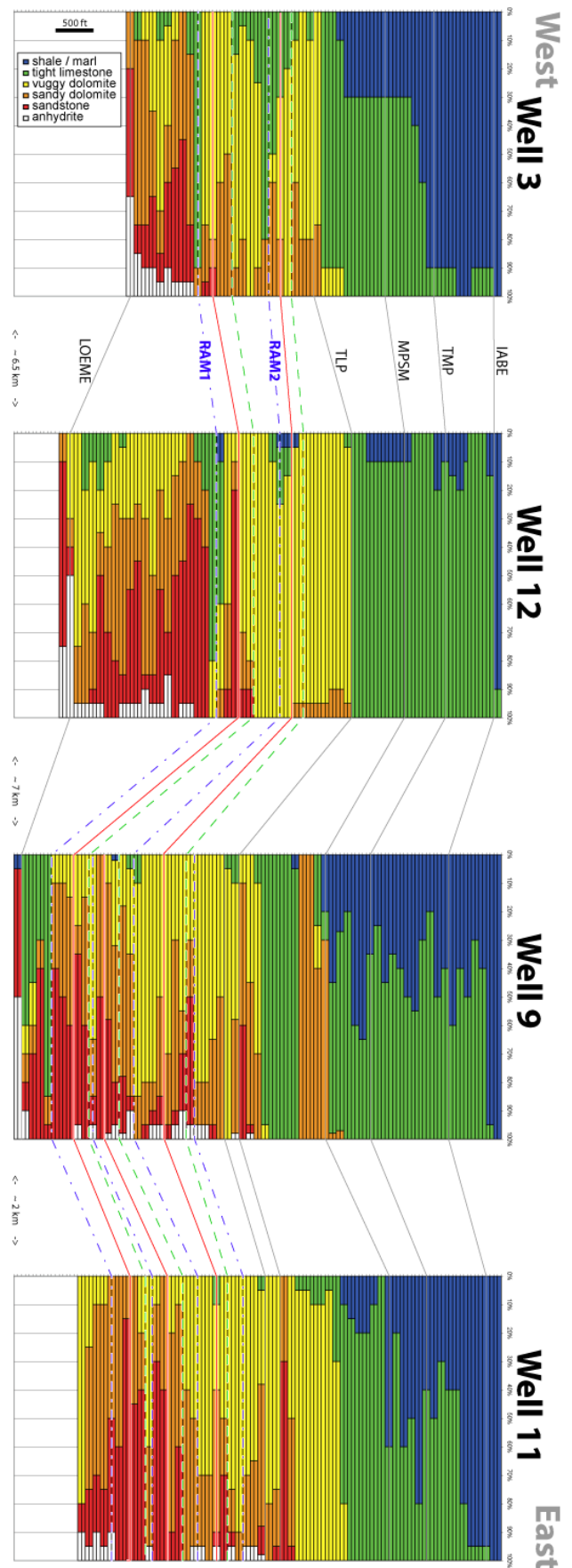
Unless calibrated and fully interpreted well logs are deemed necessary to get the best picture of the reservoirs, as for instance in EICHENSEER *et al.* (1999: Fig. 7 C), both processes are not prerequisites to correlate wells. For instance, the seismic markers of the middle-upper Pinda that are defined in the non-reservoir Moita Seca or Punja facies are easily correlated solely on the basis of log signature. One of the main features of both facies is the occurrence of rhythms, probably MILANKOVITCH'S astronomically controlled cycles, which enables us to identify new, informal, secondary markers on the well logs (Fig. 13). Such peak-to-peak correlation is eventually useful where seal facies interfinger with reservoir facies (Fig. 14).

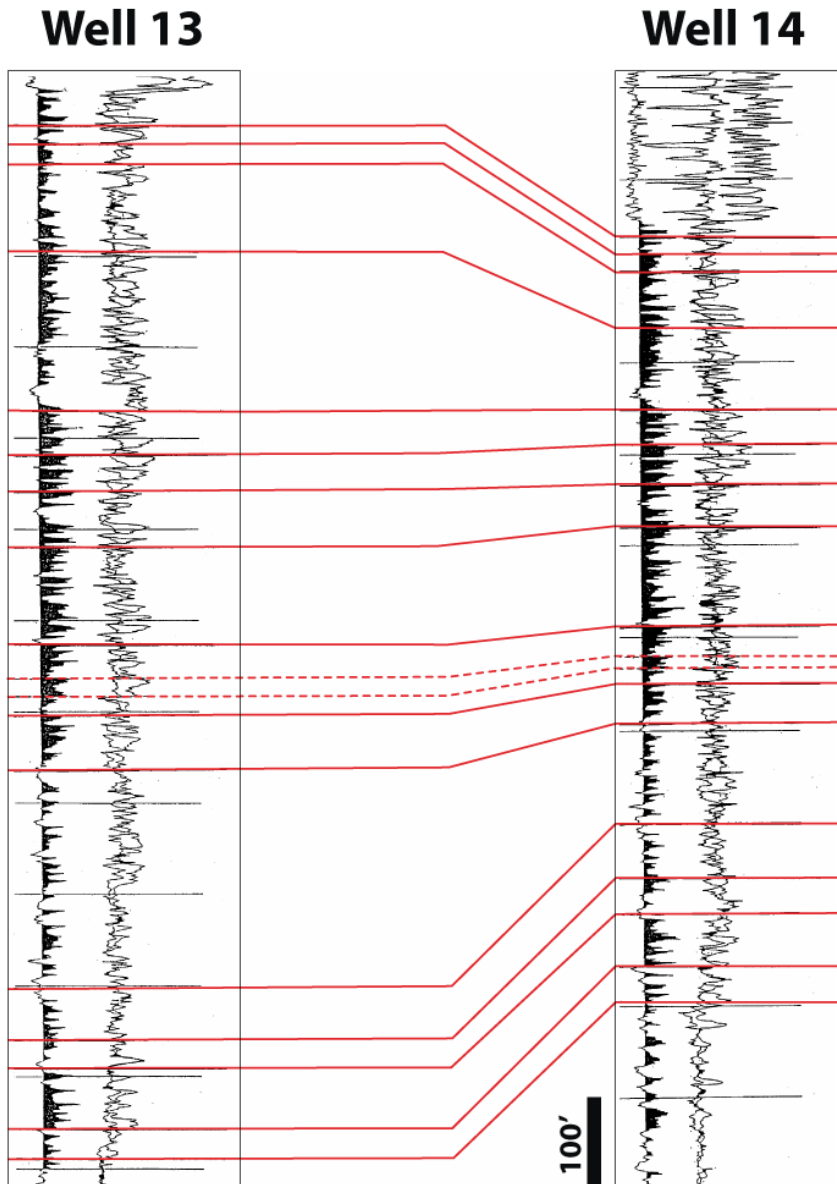
At this stage, an X-Y graph, similar to the "Line of Correlation (LoC)" diagram originally developed by SHAW (1964) for biostratigraphic correlations, may be used to cross-plot common lithologic markers between wells (*e.g.*, BUSNARDO & GRANIER, 2011). Relevant results are obtained with this technique in basinal, platform interior and ramp settings. Angolan examples will be discussed in a forthcoming publication (GRANIER, nearing completion).

The markers of the well selected as the reference well are indicated on the horizontal X axis and those of the correlated wells within the same structure or from discrete structures are plotted on the vertical Y axis. The (X,Y) dots of each well versus the reference well are connected and result in a more or less straight line. Non-linear patterns allow identification of:

- thickenings. Abrupt thickenings are commonly depositional. Gradual thickenings may indicate localized changes in the sedimentation-compaction rates;
- gaps. These may be due to normal faults or may be related to erosion or nondeposition at sequence boundaries (Figs. 15 -16).

► **Figure 12:** Correlation of computed electrofacies of wells 3, 9 and 11-12 based on Base Iabe, TMP, MPSM, TLP, 2 RadioActive Markers and Top Loeme Salt. For confidentiality purposes the name of wells and the depth scales are not provided.





◀ **Figure 13:** Peak-to-peak correlations in the upper middle and upper Pinda intervals for wells 13-14.

For confidentiality purposes the names of wells as well as the depth, GR, RhoB, and NPhi scales are not provided [RhoB and NPhi scales are reversed. From left to right, the RhoB scale runs from high to low, and the NPhi scale runs from low to high].

No angular correction is required and both vertical and deviated wells can be plotted on the diagram in the same manner. However, the apparent values of the extra or missing thicknesses should be corrected for well bore angle and bed dip effects.

When taking into account the facies of Bufalo or Pacassa reservoirs, cyclicity is still present but less easy to define due to local erosional or nondepositional gaps at sequence boundaries (SB). In this case high-resolution correlations are often a matter of interpretation (e.g., GRANIER, 1990 *et seq.*, versus EICHENSEER *et al.*, 1999). However, there are still some solid arguments: **1)** the lithologic trends, *i.e.*, coarsening- or fining-, thickening- or thinning- upward trends, and radioactivity (GR), density (RhoB), and porosity (NPhi) trends, and **2)** the points for trend reversals at transgressive surfaces (TS) and at maximum flooding surfaces (MFS). The SB identification could be a critical issue but ascri-

bing discrete HST and LST labels to the lower and upper parts of a regressive interval does not necessarily make the correlation stronger.

When taking into account the facies of Bufalo or Pacassa reservoirs, cyclicity is still present but less easy to define due to local erosional or nondepositional gaps at sequence boundaries (SB). In this case high-resolution correlations are often a matter of interpretation (e.g., GRANIER, 1990 *et seq.*, versus EICHENSEER *et al.*, 1999). However, there are still some solid arguments: **1)** the lithologic trends, *i.e.*, coarsening- or fining-, thickening- or thinning- upward trends, and radioactivity (GR), density (RhoB), and porosity (NPhi) trends, and **2)** the points for trend reversals at transgressive surfaces (TS) and at maximum flooding surfaces (MFS). The SB identification could be a critical issue but ascribing discrete HST and LST labels to the lower and upper parts of a regressive interval does not necessarily make the correlation stronger.

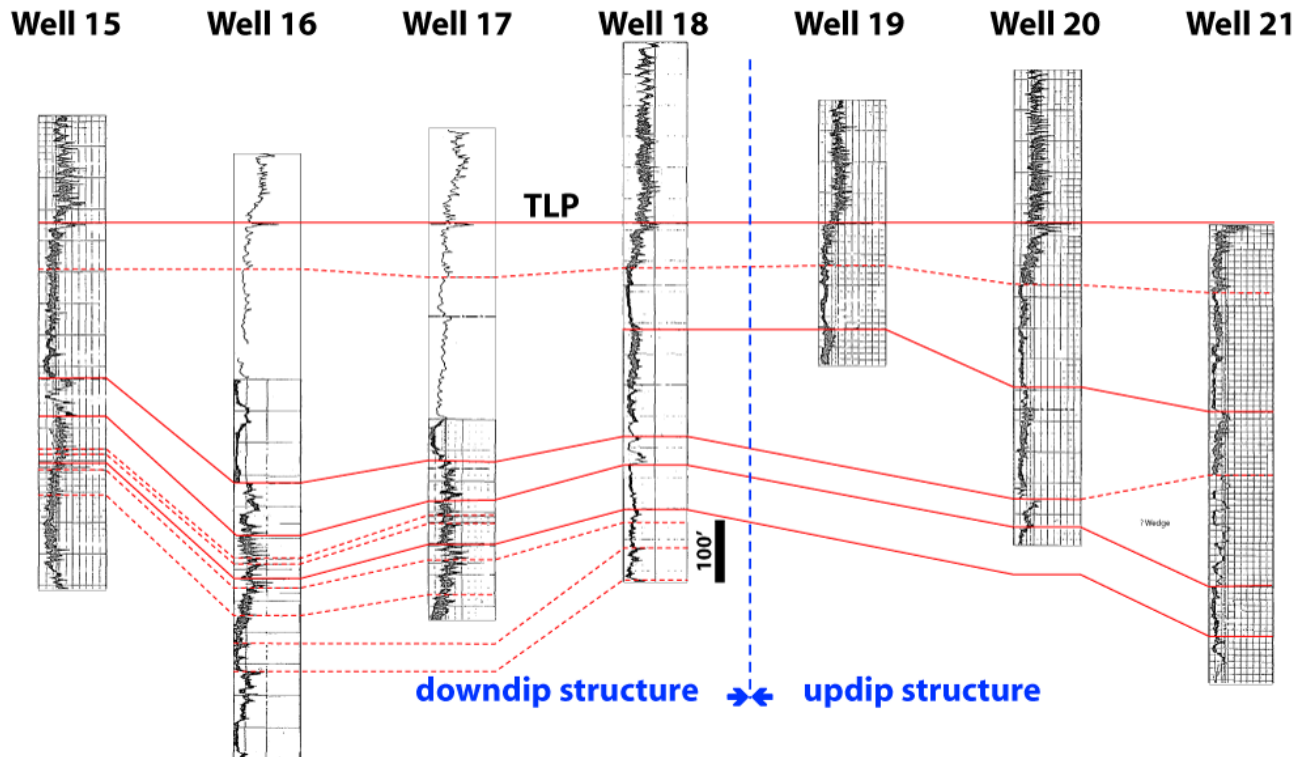


**Figure 14:** Peak-to-peak correlations in the upper lower and lower middle Pinda intervals for wells 15 to 21.

## 6. Conclusion

Integrated lithostratigraphic approaches, such as that conducted on the Pinda, always result in significant improvements in the understanding of the reservoirs. Interpretation pitfalls and dry holes, which may result from the use of seismic data only, may be avoided. Upper Aptian-Albian dolomite reservoirs, presently the Angolan Pinda dolomite reservoirs, are far better in terms of porosity and permeability than the limestone reservoirs in similar tectono-stratigraphic settings in Angola, Brazil or Congo. The integrated Pinda model drafted herein will be developed further in forthcoming publications (GRANIER, nearing completion).

## Acknowledgements

The author (B.G.) would like to thank **Sonangol** for having granted permission through an agreement dated April 13<sup>th</sup>, 2017, to use some of their material in this publication. He is very grateful to Isabel POLICARPO DA SILVA and Jean COLSOUL who acted as facilitators in the agreement with Sociedade Nacional de Combustíveis de Angola Empresa Pública – Sonangol E.P. He also acknowledges the early support of Cécile PABIAN-GOYHENECHÉ who introduced him to the geology of the Pinda Group some thirty years ago when he was doing a summer internship with elf-Aquitaine in Pau (GRANIER, 1985; PABIAN-GOYHENECHÉ *et al.*, 1986). Special thanks go to R.E. "Gene" BALLAY for comments on "quick look" interpretations of well logs and to Phil SALVADOR

for checking the final English version. Dimas DIAS-BRITO translated the abstract into Portuguese. The author is solely responsible for the interpretations and opinions expressed here, which do not necessarily reflect those of Sonangol nor of Total (or the late elf).

## Bibliographic references

- BALLAY R.E. (2014).- Eyes wide shut.- *Geo-Neurale*, Munich, 34 p. URL: <http://www.geoneurale.com/documents/EyesWideShut.pdf>
- BUSNARDO R. & GRANIER B. (2011).- Aptian ammonites of Abu Dhabi (United Arab Emirates) [Ammonites aptiennes d'Abou Dabi (Émirats Arabes Unis)].- *Carnets Geol.*, Madrid, vol. 11, no. L04 (CG2011\_L04), p. 117-135.
- EICHENSEER H.T., WALGENWITZ E R. & BIONDI P.J. (1999).- Stratigraphic control on facies and diagenesis of dolomitized sequences (Pinda Group, Albian, offshore Angola).- *AAPG Bulletin*, vol. 83, no. 11, p. 1729-1758.
- FERRÉ B. & GRANIER B. (2001).- Albian roveacrinids from the southern Congo Basin off Angola.- *Journal of South American Earth Sciences*, vol. 14, p. 219-235.
- GRANIER B. (1985, unpublished).- Codification macrolithologique de carottes appliquée à l'étude du réseau macroporeux - Application au réservoir Pinda inférieur du champ de Palanca (Angola).- Société Nationale elf-Aquitaine (Production), Rapport de Stage, Pau, 28 p.

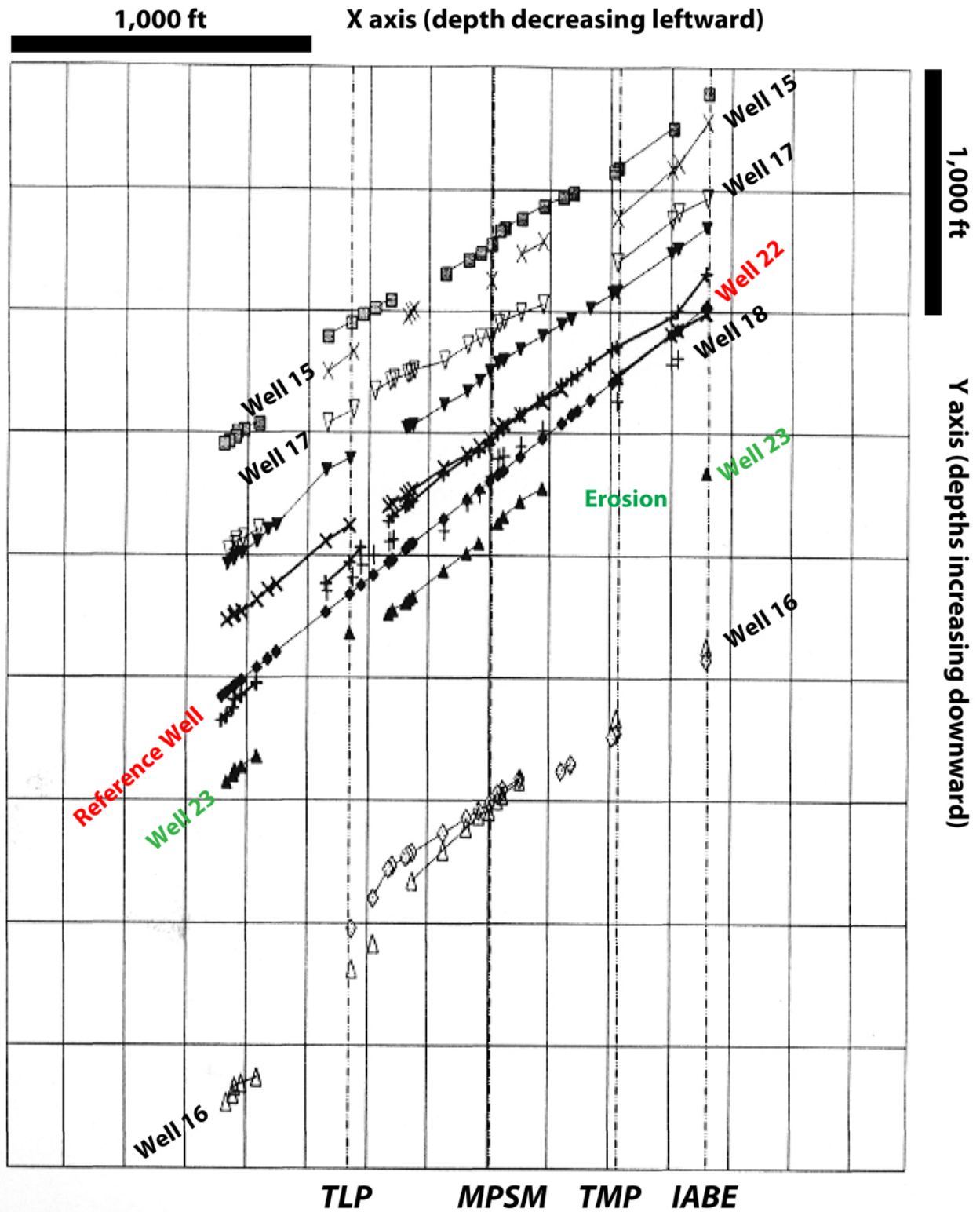


**Figure 15:** LoC for wells of one structure (see comments in the text). The reference well (well 22) corresponds to the grey rectangles and well 23 to the white triangles. The erosion at the top of the Pinda in well 23 can be estimated at approximately 500 feet (this value has to be corrected for both the borehole deviation and the structural dip angle). Vertical and horizontal depth scales are given in thousands of feet. For confidentiality purposes the names of wells and the depth scales are not provided.

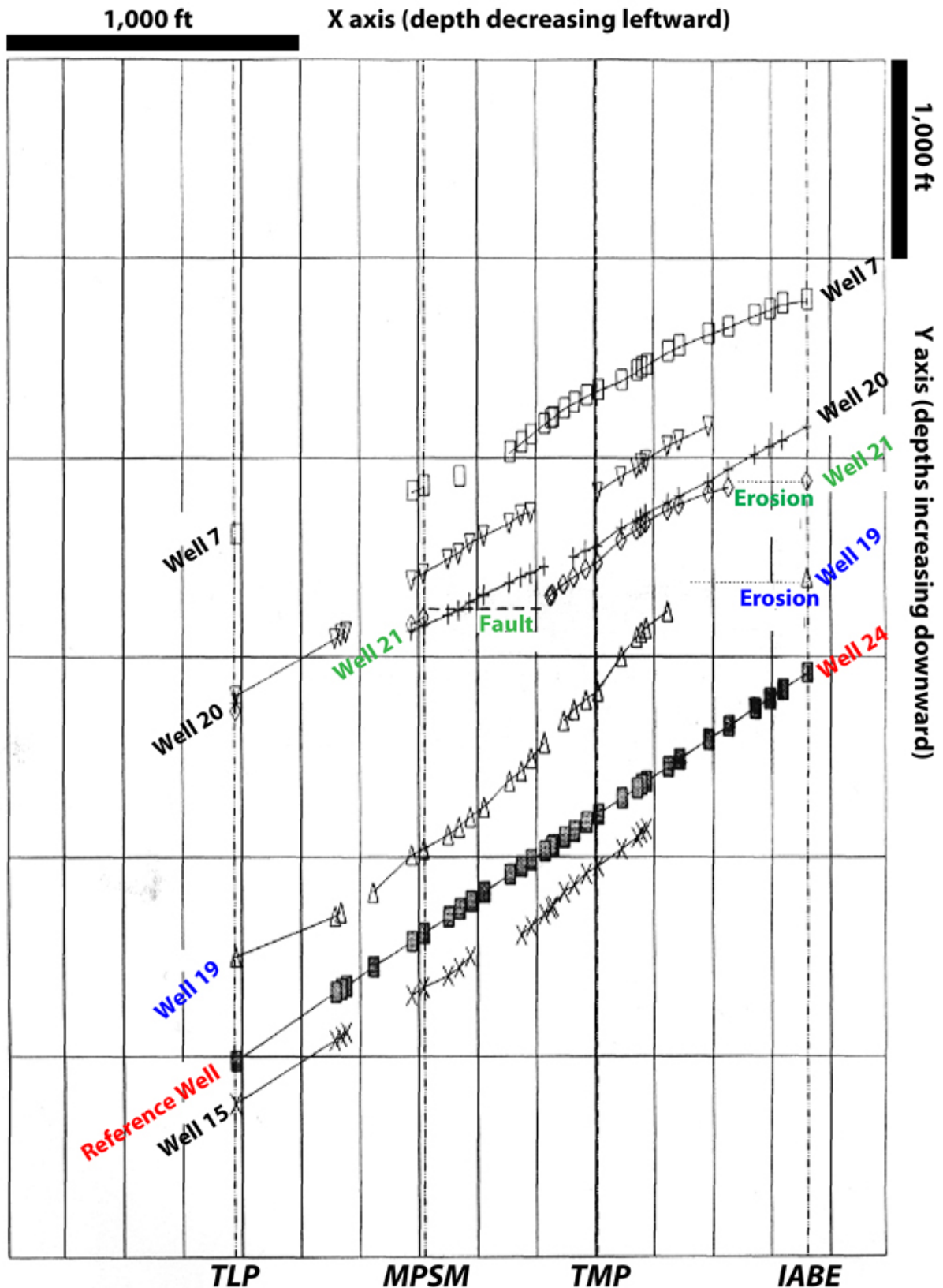


**Figure 16:** LoC for wells of another structure (see comments in the text). The reference well (well 24) corresponds to the grey rectangles, well 19 to the white triangles and well 21 to the white diamonds. The erosion at the top of the Pinda in wells 19 and 21 can be estimated at approximately 500 and 200 feet respectively. In addition, due to a fault occurrence in well 21, approximately 200 feet of upper middle Pinda section are missing (these values have to be corrected for both the borehole deviation and the structural dip angle). Vertical and horizontal depth scales are given in thousands of feet.



- GRANIER B. (1990, unpublished).- Nouvelle nomenclature stratigraphique (séquentielle) de l'Albien de l'offshore angolais. Implications sédimentologiques et structurales.- Rapport SCOP 6, Société Nationale elf-Aquitaine (Production), Pau, 14 p.
- GRANIER B. (1991a, unpublished).- Application des concepts de la stratigraphie séquentielle à l'étude des réservoirs albiens (Pinda) du bloc 2, Angola.- Total, Saint-Rémy-lès-Chevreuse, Mémo CST/CARB 91-129.
- GRANIER B. (1991b, unpublished).- Tentative d'établissement d'un modèle sédimentologique du Pinda sur la moitié sud du bloc 2, offshore angolais (60 puits).- Total, Saint-Rémy-lès-Chevreuse, Mémo CST/CARB 91-208.
- GRANIER B. (1992, unpublished).- Tentative d'établissement d'un modèle sédimentologique du Pinda (Albo - ? Cénomaniens) sur la moitié sud du bloc 2 (50 puits), offshore angolais.- Total, Rapport Laboratoires no. 4850, Saint-Rémy-lès-Chevreuse, vol. I (text): 28 p.; vol. II (figures and appendices).
- GRANIER B. & DIAS-BRITO D. (2016).- On the fossil alga *Marinella lugeoni* PFENDER, 1939, *nom. cons.*, and its seven unfortunate avatars. Revision of the Juliette PFENDER Collection. Part 2. Revision of the Jesse Harlan JOHNSON Collection. Part 2.- *Carnets Geol.*, Madrid, vol. 16, no. 7, p. 231-245.
- GRANIER B. & GOY G. (1993, unpublished).- Pinda Formation, Block 2, Offshore Angola. Catalogue of microfacies of the Lower and Middle Pinda Formation, based on the cored intervals from 22 wells.- Total, Rapport Laboratoires no. 5143, Saint-Rémy-lès-Chevreuse, 10 p. (50 Pls.).
- GRANIER B., GOY G. & IMBERT P. (1993, unpublished).- Pinda Formation, Block 2, Offshore Angola. Regional overview, based on the (re)appraisal of core analyses from 22 wells.- Total, Rapport Laboratoires no. 5126, Saint-Rémy-lès-Chevreuse, vol. I (text): 56 p. ; vol. II (appendices); vol. III (11 Pls.).
- KOCHHANN K.G.D., KOUTSOUKOS E.A.M., FAUTH G. & STAL A.N. (2013).- Aptian - Albian planktic foraminifera from DSDP Site 364 (offshore Angola): biostratigraphy, paleoecology, and paleoceanographic significance.- *Journal of Foraminiferal Research*, Lawrence, vol. 43, no. 4, p. 443-463.
- KOUTSOUKOS E.A.M., MELLO M.R., FILHO N.C. de AZAMBUJA, HART M.B. & MAXWELL J.R. (1991).- The upper Aptian-Albian succession of the Sergipe basin, Brazil: an integrated paleoenvironmental assessment.- *AAPG Bulletin*, vol. 75, no. 3, p. 479-498.
- MASSE P. (1995).- Calcareous algae and microprolites of the Albian platform carbonates of the Congo margin.- *Bulletin du Centre de Recherches Exploration-Production elf-Aquitaine*, Pau, vol. 19, no. 2, p. 301-317.
- MATHIS B. (1993).- Well logging and diagenesis: case studies and new means of research.- *Bulletin du Centre de Recherches Exploration-Production elf-Aquitaine*, Pau, vol. 17, no. 2, p. 385-393.
- PABIAN-GOYHENECHÉ C., SEHANS P. & GRANIER B. (1986, unpublished).- Gisements du Pinda d'Angola (Volet Géologie). Codification lithologique et microtectonique de carottes appliquée au réseau poreux du réservoir carbonaté vacuolaire de Palanca.- Société Nationale elf-Aquitaine (Production), Rapport EP/S/EXP/RAG/Lab.Pau no. 86/138RS, 20 p.
- ROMANES M.F. (1916).- XVI. Note on an algal limestone from Angola.- *Transactions of the Royal Society of Edinburgh*, vol. LI, part III, no. 16, p. 581-584 (Pl.).
- SHAW A.B. (1964).- Time in stratigraphy.- McGraw-Hill, New York, 365 p.
- STARK D.M. (ed., 1991).- Avaliação de formações de Angola.- *Well Evaluation Conference*, Schlumberger, 95 + 55 + 73 + 66 + 40 p.

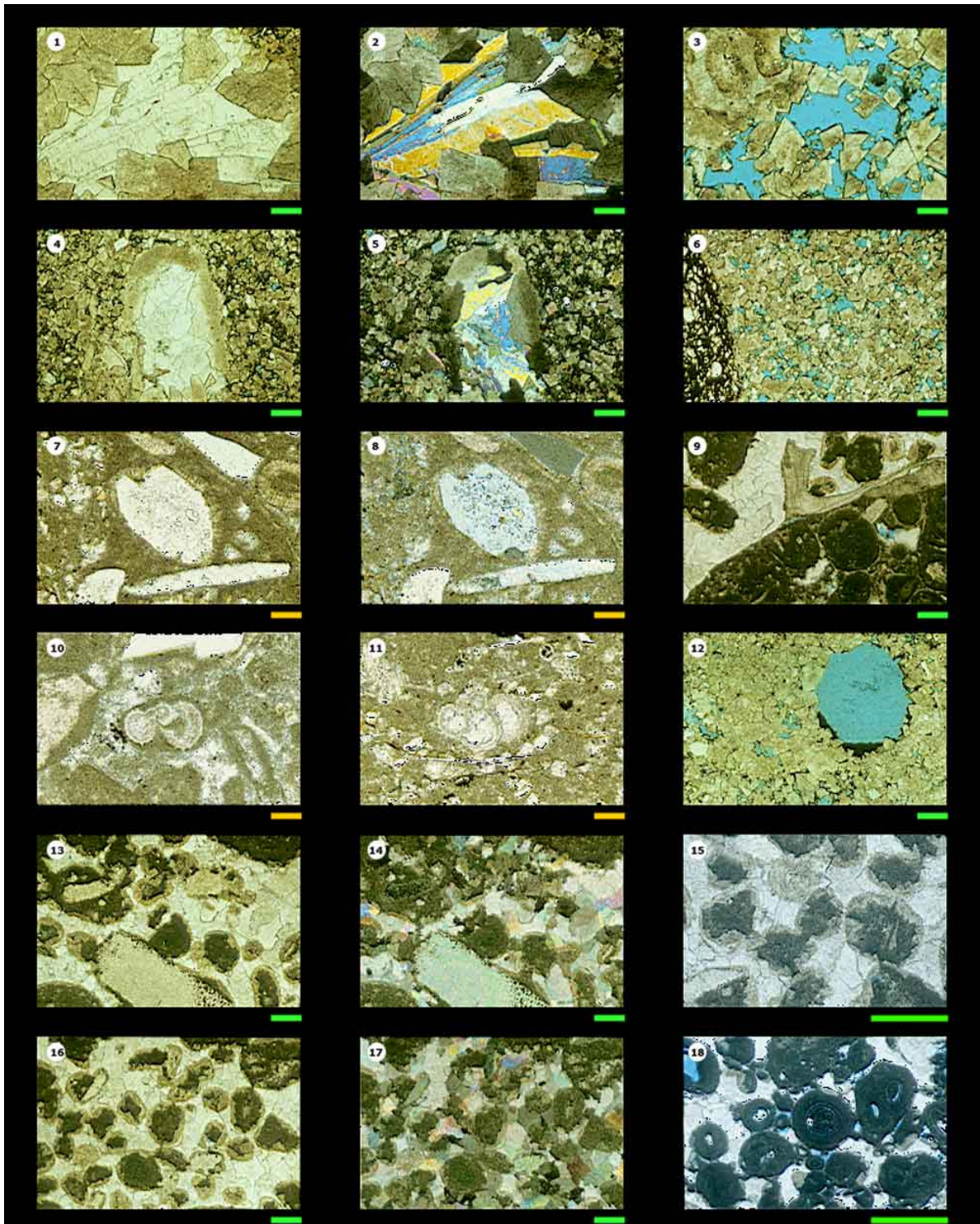


**Plate 1:** 1. baroque dolomite and anhydrite cement, TL; 2. as above, PL; 3. dolograinstone with a dolomitized gastropod shell. Porosity is intercrystalline to vuggy, TL; 4. echinid cavity infilled with anhydrite cement, TL; 5. as above, PL; 6. dolograinstone with intercrystalline porosity, TL; 7. quartz grain with salt-rich inclusions, TL; 8. as above, PL; 9. lithoclast encrusted by oysters, TL; 10. *Favusella washitensis*, TL; 11. *Favusella washitensis*, TL; 12. dolograinstone with intercrystalline and vuggy (moldic) porosity. Bitumen, TL; 13. partly dolomitized oolitic grainstone with echinoderm remains, TL; 14. as above, PL; 15. partly dolomitized oolitic grainstone, TL; 16. partly dolomitized oolitic grainstone, TL; 17. as above, PL; 18. partly dolomitized oolitic grainstone, TL.

Scale bars: green 500  $\mu\text{m}$ ; orange 125  $\mu\text{m}$ . TL transmitted light; PL polarized light (analyzed); RL reflected light; CL cathodoluminescence. For confidentiality purposes the sample depths and the name of wells are not provided.

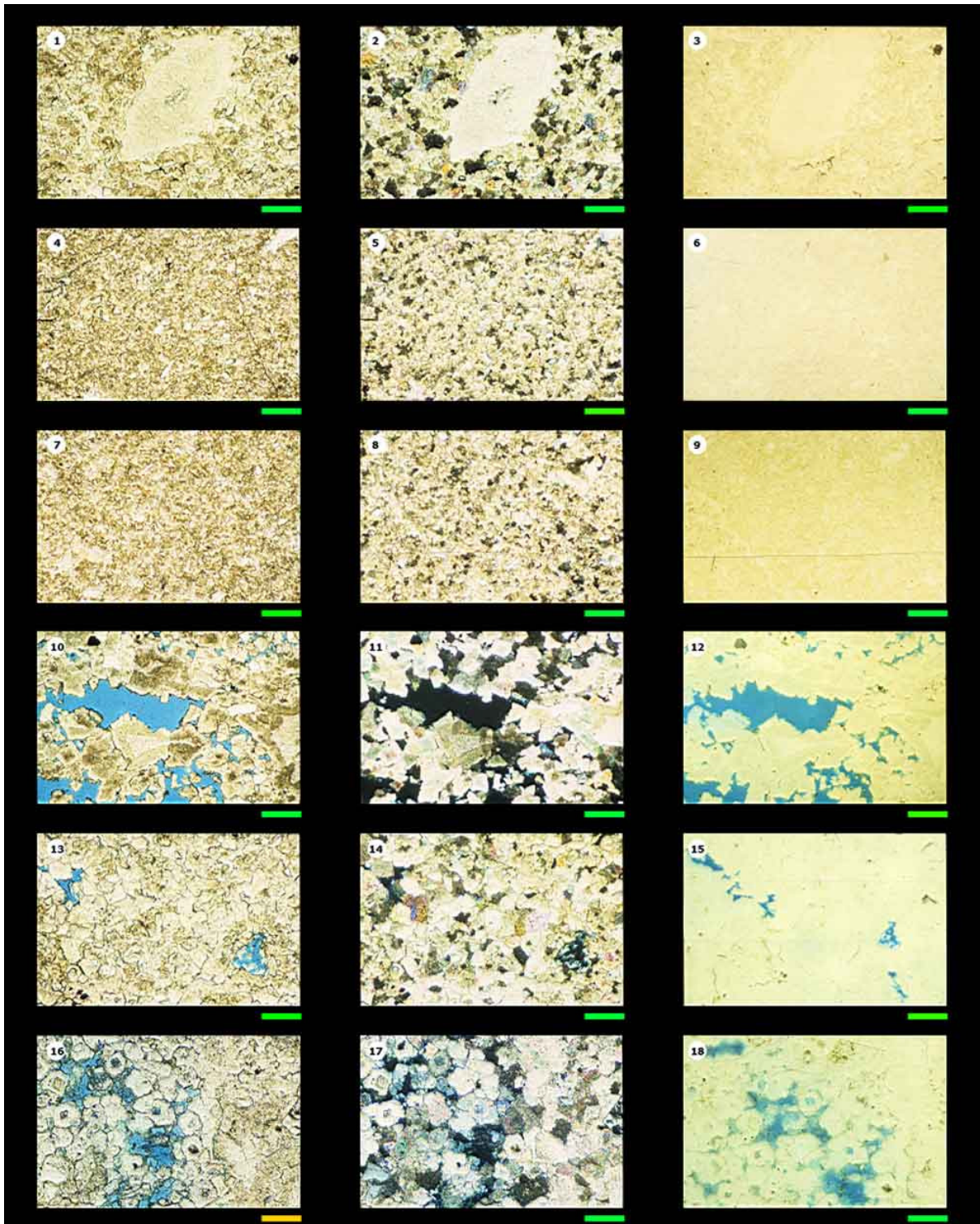


**Plate 2:** 1. dolograins (sucrosic mosaic) with echinoid spine, TL; 2. as above, PL; 3. as above, RL; 4. fine dolograins, TL; 5. as above, PL; 6. as above, RL; 7. fine dolograins, TL; 8. as above, PL; 9. as above, RL; 10. dolograins with moldic porosity, TL; 11. as above, PL; 12. as above, RL; 13. dolograins with moldic porosity, TL; 14. as above, PL; 15. as above, RL; 16. intracrystalline porosity, TL; 17. as above, PL; 18. as above, RL.

Scale bars: green 500  $\mu\text{m}$ ; orange 125  $\mu\text{m}$ . TL transmitted light; PL polarized light (analyzed); RL reflected light; CL cathodoluminescence. For confidentiality purposes the sample depths and the name of wells are not provided.

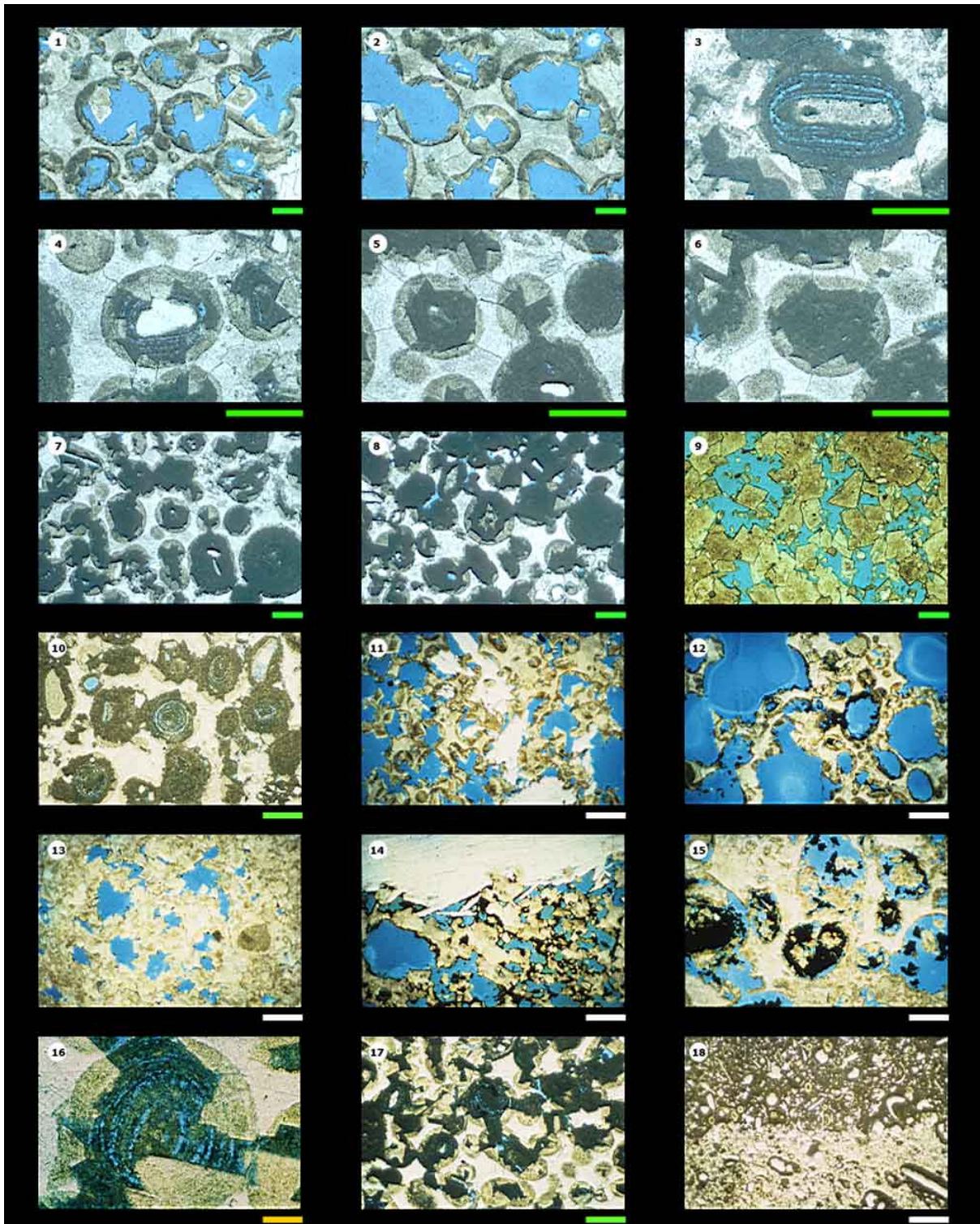


**Plate 3:** 1. dolograins with moldic porosity, TL; 2. dolograins with moldic porosity, TL; 3. micritic ooid in a partly dolomitized oolitic grainstone, TL; 4. partly dolomitized oolitic grainstone, TL; 5. partly dolomitized oolitic grainstone, TL; 6. partly dolomitized oolitic grainstone, TL; 7. partly dolomitized oolitic grainstone, TL; 8. partly dolomitized oolitic grainstone, TL; 9. dolograins with intercrystalline porosity, TL; 10. partly dolomitized oolitic grainstone, TL; 11. dolograins with moldic porosity and anhydrite cement, TL; 12. dolograins with moldic porosity. Bitumen, TL; 13. dolograins with intercrystalline and moldic porosity, TL; 14. dolograins with intercrystalline and moldic porosity, and anhydrite cement. Bitumen, TL; 15. dolograins with moldic porosity. Bitumen, TL; 16. micritic ooid in a partly dolomitized oolitic grainstone, TL; 17. partly dolomitized oolitic grainstone, TL; 18. contact between a dolomitized and non dolomitized facies, TL.

Scale bars: white 1000 $\mu$ m; green 500  $\mu$ m; orange 125  $\mu$ m. TL transmitted light; PL polarized light (analyzed); RL reflected light; CL cathodoluminescence. For confidentiality purposes the sample depths and the name of wells are not provided.

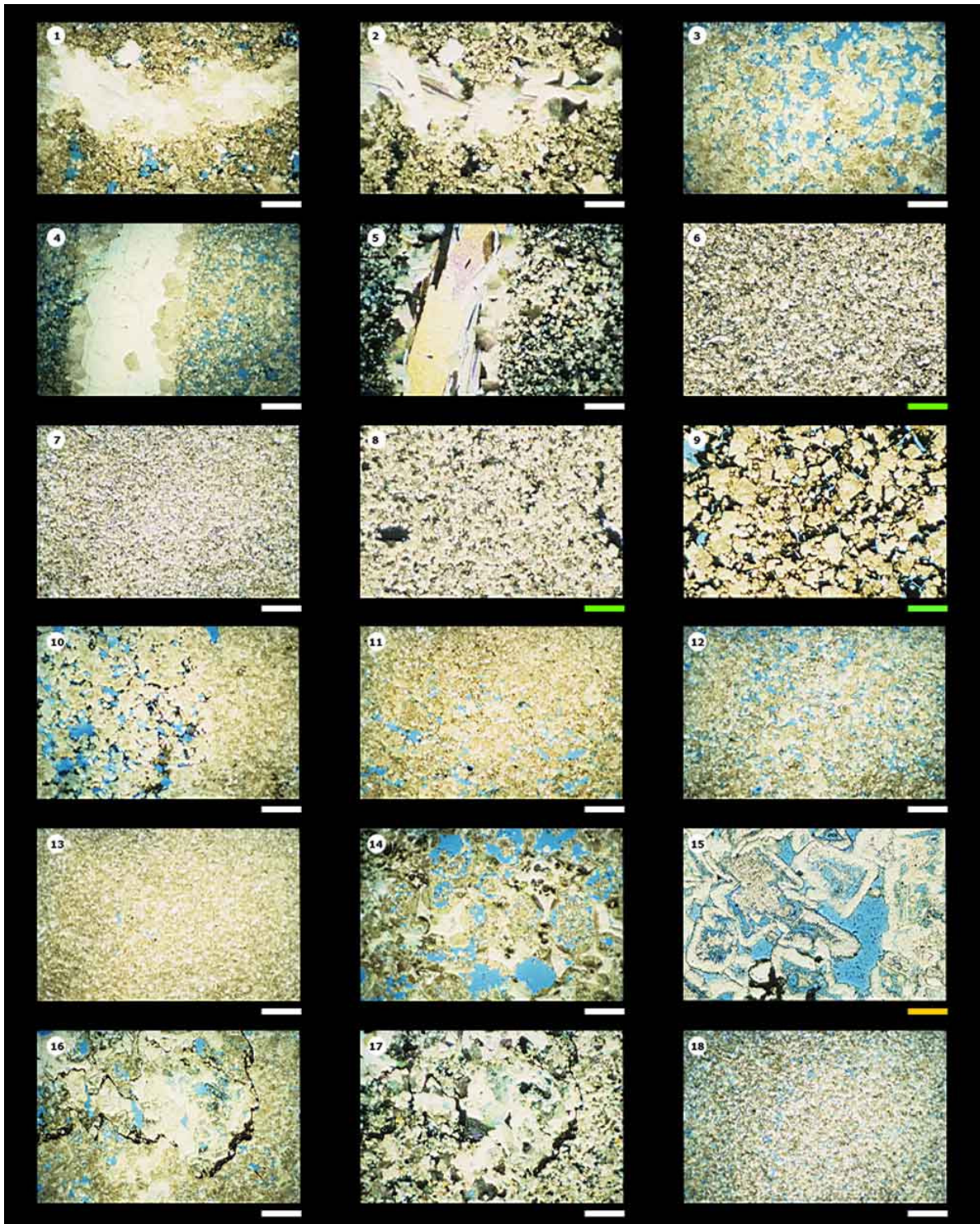


**Plate 4:** 1. anhydrite cement, TL; 2. as above, PL; 3. dolograinstone with intercrystalline porosity, TL; 4. anhydrite cement, TL; 5. as above, PL; 6. silty mudstone with intercrystalline porosity, TL; 7. silty mudstone, TL; 8. silty mudstone, TL; 9. dolograinstone with intercrystalline porosity. Bitumen, TL; 10. dolograinstone with intercrystalline porosity, TL; 11. fine dolograinstone with intercrystalline porosity, TL; 12. fine dolograinstone with intercrystalline porosity, TL; 13. silty mudstone, TL; 14. dolograinstone with intercrystalline and moldic porosity, TL; 15. intracrystalline porosity, TL; 16. stylolites in dolograinstone, TL; 17. as above, PL; 18. silty mudstone, TL.

Scale bars: white 1000µm; green 500 µm; orange 125 µm. TL transmitted light; PL polarized light (analyzed); RL reflected light; CL cathodoluminescence. For confidentiality purposes the sample depths and the name of wells are not provided.

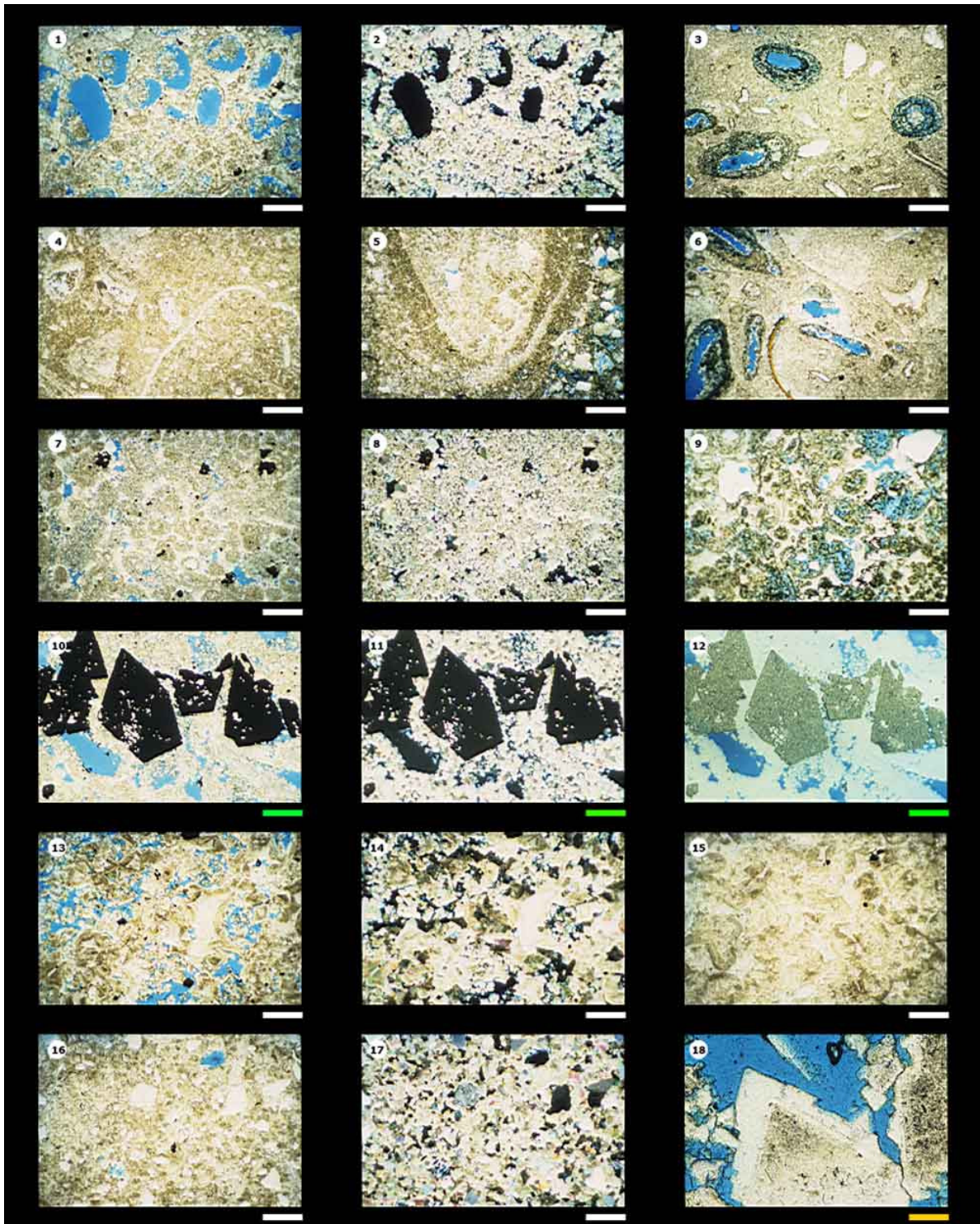


**Plate 5:** 1. dolograinstone with intercrystalline and moldic porosity, TL; 2. as above, PL; 3. dolowackestone with moldic porosity, TL; 4. pelecypod, TL; 5. pelecypod, TL; 6. dolowackestone with pelecypods and oncoids, TL; 7. dolograinstone with intercrystalline porosity, TL; 8. as above, PL; 9. dolograinstone with intercrystalline and moldic porosity, TL; 10. pyrite, TL; 11. as above, PL; 12. as above, RL; 13. dolograinstone with intercrystalline and moldic porosity, TL; 14. as above, PL; 15. tight dolograinstone, TL; 16. sandy dolograinstone with intercrystalline and moldic porosity, TL; 17. as above, PL; 18. dolomite crystal showing both replacement and cement stages, TL.

Scale bars: white 1000µm; green 500 µm; orange 125 µm. TL transmitted light; PL polarized light (analyzed); RL reflected light; CL cathodoluminescence. For confidentiality purposes the sample depths and the name of wells are not provided.

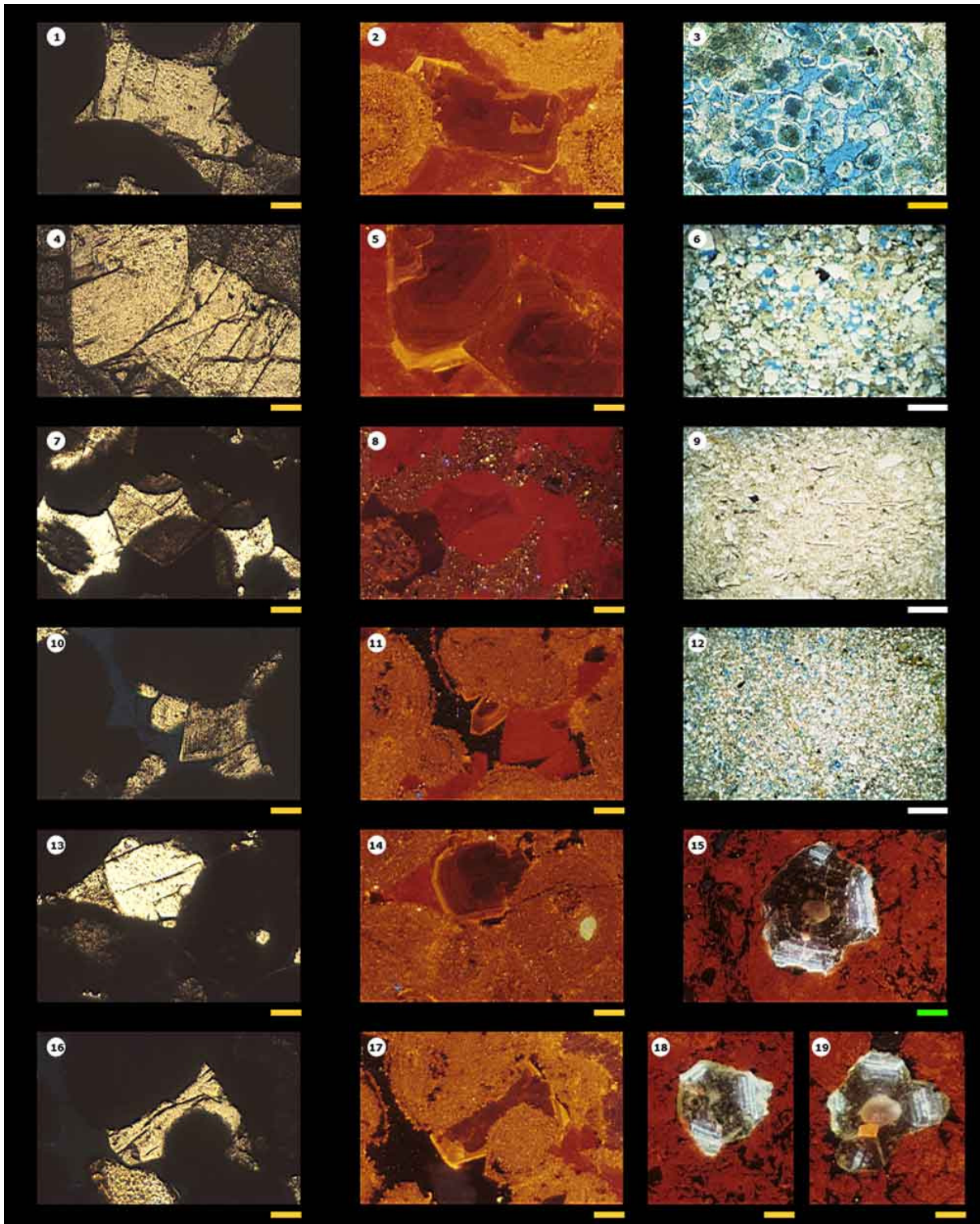


**Plate 6:** 1. calcite and dolomite cement in an intergranular position, TL; 2. as above, CL; 3. intracrystalline porosity, TL; 4. calcite and dolomite cement in an intergranular position, TL; 5. as above, CL; 6. sandy dolograins with intercrystalline porosity, TL; 7. dolomite cement in an intergranular position, TL; 8. as above, CL; 9. silty dolomudstone, TL; 10. calcite and dolomite cement in an intergranular position, TL; 11. as above, CL; 12. silty dolomudstone with intercrystalline porosity, TL; 13. calcite and dolomite cement in an intergranular position, TL; 14. as above, CL; 15. sphalerite (considered to be of hydrothermal origin), CL; 16. calcite and dolomite cement in an intergranular position, TL; 17. as above, CL; 18. sphalerite, CL; 19. sphalerite, CL.

Scale bars: white 1000µm; green 500 µm; orange 125 µm. TL transmitted light; PL polarized light (analyzed); RL reflected light; CL cathodoluminescence. For confidentiality purposes the sample depths and the name of wells are not provided.

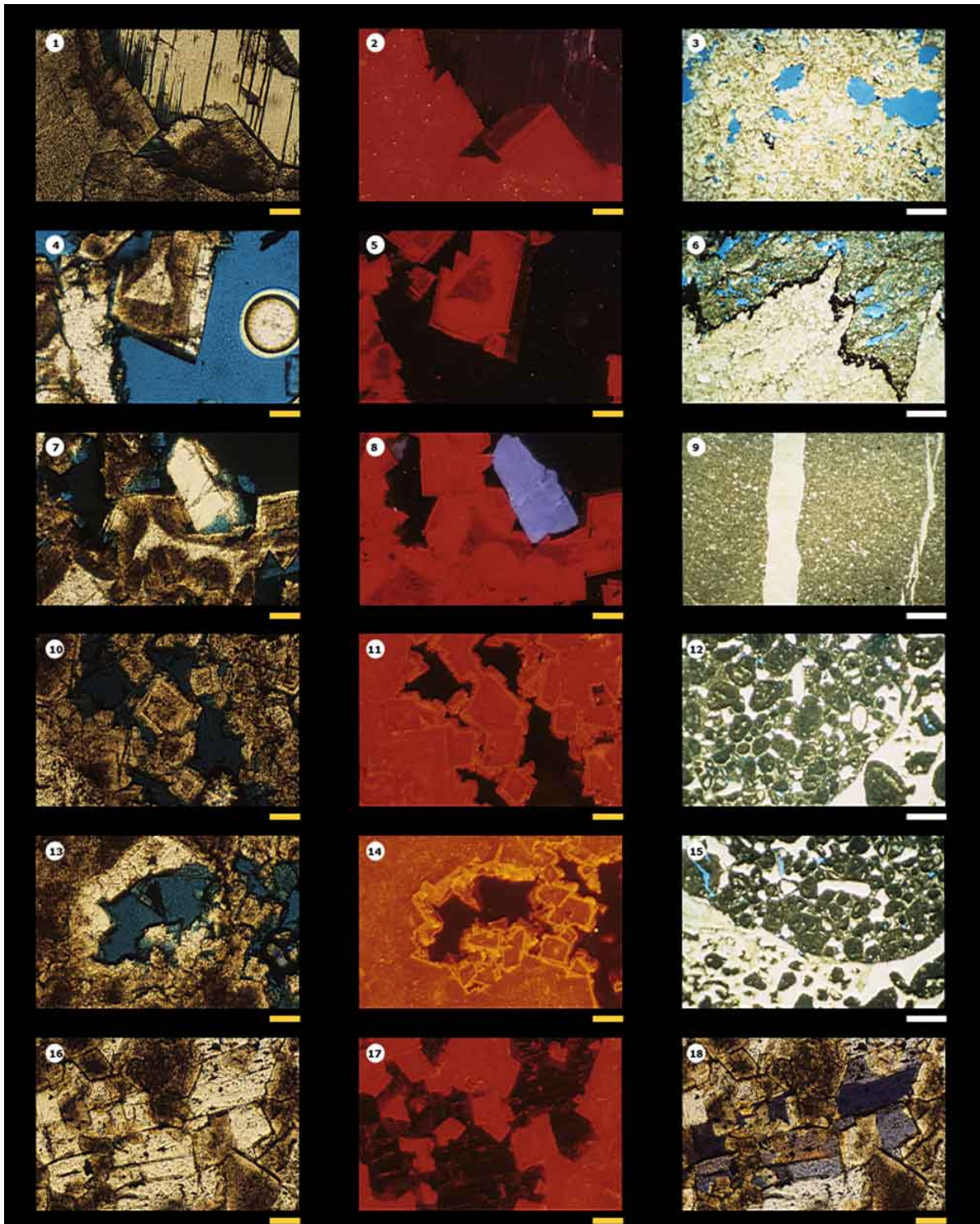


**Plate 7:** 1. anhydrite and dolomite crystals showing both replacement and cement stages, TL; 2. as above, CL; 3. dolograins with moldic porosity, TL; 4. dolomite crystal showing both replacement and cement stages, TL; 5. as above, CL; 6. stylolite, TL; 7. feldspar and dolomite crystal showing both replacement and cement stages, TL; 8. as above, CL; 9. dolomudstone with cemented fracture, TL; 10. zoned dolomite crystals, TL; 11. as above, CL; 12. lithoclast, TL; 13. zoned dolomite crystals, TL; 14. as above, CL; 15. lithoclast, TL; 16. dolomite crystals cemented by anhydrite, TL; 17. as above, CL; 18. as above, PL.

Scale bars: white 1000 $\mu$ m; orange 125  $\mu$ m. TL transmitted light; PL polarized light (analyzed); RL reflected light; CL cathodoluminescence. For confidentiality purposes the sample depths and the name of wells are not provided.